DESIGN OF APPROPRIATE WAVELET BASES FOR TEXTURE DISCRIMINATION

By

Mohammad Ali Chaudhry

Submitted to the Department of Electrical Engineering, Military College of Signals, in partial fulfillment of the requirements for the degree of Doctor of Philosophy

National University of Sciences and Technology
Rawalpindi, Pakistan

September 2007

DESIGN OF APPROPRIATE WAVELET BASES FOR TEXTURE DISCRIMINATION

Approved for the Department of Electrical Engineering, Military College of Signals, National University of Sciences and Technology.

Supervisor:	_____ Dr. M.Noman Jafri
Co-supervisor:	_____ Dr. Muid Mufti
Chairman of the examination committee:	_____ Dr. Muhammad Akbar
Date:	_____

ABSTRACT

DESIGN OF APPROPRIATE WAVELET BASES FOR TEXTURE DISCRIMINATION

Problem of texture analysis and discrimination using wavelet transform has been under consideration for the last three decades by several researchers from different fields. Unlike Fourier transform, several bases are available in wavelet transform for signal decomposition, but none of these has been designed by considering the actual texture images to be discriminated. Therefore, a system is required for the design of wavelet bases which caters the actual texture image to be discriminated. There are several factors involved in wavelet design which can greatly influence the desired results such as regularity, length of the wavelet, orthogonal or biorthogonal etc.

In this research work, we have analyzed different regions of Pakistan on the basis of their textural properties. We propose a design of wavelet bases using genetic optimization, which will provide excellent discrimination between the multiple texture images. Our objective function is based on maximization of distinguishability measure involving the computation of finer details subject to some wavelet constraints. In contrast to well known orthogonal wavelet families, we have used extra degree of freedom in design of the wavelet function for best possible texture discrimination. In genetic optimization process, design parameters of wavelet are optimized according to the characteristics of texture images under defined set of constraints. Classification results of optimized orthogonal and biorthogonal wavelet were compared with the existing wavelet families, which show that the results obtained are superior in terms of texture discrimination. The proposed system is

capable of designing optimized wavelet by changing the input texture images for different applications such as medical images, satellite images, document analysis and industrial application etc.

TO MY PARENTS

AKNOWLEDGEMENTS

I would like to take this opportunity to express my sincerest gratitude to all those who have assisted me throughout the last few years. It is the many mentors, friends and colleagues who have not only made my Ph.D. research possible, but also tremendously rewarding and enjoyable.

Firstly, I would like to thank my principal supervisor and respected teacher, Professor Dr. Mohammad Noman Jafri. Completion of research work and thesis would not have been possible without his guidance and he has proved to be a continual source of inspiration and encouragement.

I would also like to thank Professor Dr. Muid Mufti (University of Engg & Technology, Taxila Pakistan), who co-supervised my research work during the entire phase of my Ph.D research. His friendly encouragement and guidance eased me into the challenges of research work.

Last but not the least, I would like to thank chief instructor at College of Signals Dr. Muhammad Akbar for his timely technical guidance and continuous administrative support throughout my stay at the university. I would like to thank Dr. Saleem Akbar and Dr. Saeed Murtaza for his encouraging remarks from time to time.

I pay sincere gratitude to Higher Education Commission for providing financial assistance and also to my parent department KRL for sparing me for higher studies.

TABLE OF CONTENTS

LIST OF TABLES

LIST OF FIGURES

CHAPTER 1

INTRODUCTION

Texture analysis has been an important field in computer vision and under intense investigation by numerous researchers from different field for the past several years. Most of the natural surfaces exhibit textural characteristics hence, texture analysis and recognition system will be a natural part of many computer vision systems. Therefore, texture is an important characteristic for the analysis of many types of images. Several techniques have been proposed for texture analysis and discrimination, but none of them proved to be a benchmark in the field, because of different underlying textural properties. Therefore, texture analysis remains a fundamental problem in computer vision.

1.1 Motivation and Problem Definition

Texture in an image generally refers to a region with certain variation of intensities, which form fineness and coarseness, and have some repetitive patterns as well. It can not be defined by its shape, size or edges etc, but can be recognized by its primitives and attributes. Several techniques have been developed in the past. The techniques can roughly be divided into four categories such as Statistical, Geometrical, Model based and Signal processing [1].

Most of the early methods exploit inter pixel relationship and features are extracted in the spatial domain, which may or may not be enough for texture analysis. Appearance of repetitive patterns in texture images corresponds to presence of different

frequency components. Frequencies and their strength can best be analyzed by using signal processing methods, especially using decomposition of texture image into different frequency resolution scales.

More recent techniques involve the use of a variable-scale analysis of textured images. The main advantage of this approach is that it is capable of zooming to arbitrary scales in the analysis, thus allowing examination of textures at their appropriate scales. Even within a homogeneous texture, there may be important defining characteristics at more than one scale. Hence, these approaches are often called filter-based or multi-channel filtering approaches. Early incarnation of these methods use Gabor filters at different scales to characterize textures. More recently, these approaches have evolved to encompass the use of the wavelets [1, 2].

The wavelet is the most widely natural mathematical tool to use for this purpose because of its inherent multiresolution properties. Wavelet analysis is a versatile tool with compact and comprehensive mathematical formulation and therefore, has broad applications such as signal processing, image analysis, communication systems etc. A lot of research and achievements have been made in the field of textural feature extraction by using wavelet analysis. However, the avenues of research on applying the wavelets to texture analysis are in an exploratory stage.

In case of Fourier transform, several types of wavelets are available for signal decomposition. However, it is not possible to determine which wavelet would provide the optimum results. Therefore, this open question emphasizes the need of intelligent system, which can efficiently discriminate the given class of textured images.

1.2 Aims of Thesis

Texture analysis can be divided into two sub-categories: classification and segmentation. These two problems share common attributes and techniques. Segmentation and classification may primarily be based upon the quality of discriminant textural features extracted by an artificial vision system.

In this research work, we propose a scheme for the design of a wavelet bases for texture discrimination using genetic algorithms as shown in Figure 1.1. In the genetic optimization process, design parameters of the wavelet are optimized according to the characteristics of the texture images. Necessary and sufficient conditions for designing orthogonal and biorthogonal wavelet were kept as constraints in optimization process.

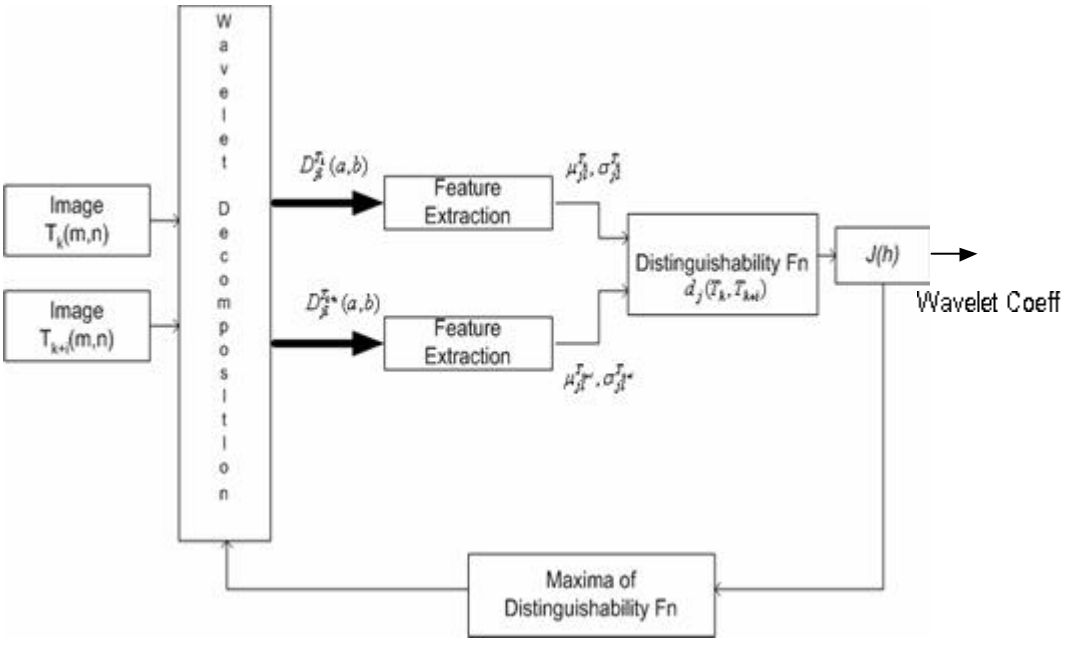

Figure 1.1 Learning System Block Diagram

Designed wavelet maximizes the distinguishability function by moving the feature vectors of different textures apart with respect to a reference image, thus giving best

possible texture discrimination. In this technique, single mother wavelet function is required for a particular set of texture images which reduces the computational complexity. Experimental analysis has been carried out using remotely sensed texture images of Pakistan and wavelet function was optimized to illustrate the discrimination capability of the proposed technique.

1.3 Organization of Thesis

In Chapter 2, different techniques for textural feature extraction have been discussed in detail, we have mainly emphasized on techniques related to statistical and signal processing domain.

In Chapter 3, multiresolution and wavelet theory has been discussed along with its necessary and sufficient conditions for the design of wavelet bases. In later part of this chapter, detailed survey is presented on applications related to wavelet in the field of texture analysis and discrimination.

A methodology is proposed in Chapter 4 for the design of wavelet bases using genetic optimization, which will provide excellent discrimination between the multiple texture images. In the genetic optimization process, design parameters of wavelet are optimized according to the characteristics of the texture images under defined set of constraints. Finally, results of designed wavelet are given in Chapter 5. We have analyzed different regions of Pakistan on the basis of their textural properties and found that our results are superior to other well known wavelet families in term of texture discrimination.

CHAPTER 2

TEXTURE FEATURE EXTRACTION

2.1 Introduction

Texture is a widely used and implicitly understandable term; it is easy to recognize but hard to define. Texture involves spatial distribution of intens ity levels in certain pattern, it may be considered as a repetitive pattern. In the Webster dictionary, texture is defined as "the character of a surface as determined by the arrangement, size, quality" or "the arrangement of particles or constituent parts of any material as it affects the appearance or feel of the surface". Humans usually describe a given texture by words like fine, coarse, smooth, rough etc. These attributes are again instinctually obvious, however still relative and not easily measurable. In this chapter, different techniques of texture analysis and discrimination are discussed.

2.2 Texture Analysis

Robust texture analysis is an important task for classification and segmentation of textured regions in an image and it is based upon the quality of extracted features. For successful classification, it is equally important to describe their *(micro-textures)* local and *(macro-textures)* global characteristics. Local characteristics correspond to inter-pixel relation, which are best described by the statistical techniques, and global characteristics correspond to repeated patterns in an image. Most widely used techniques in the field of texture analysis are statistical and signal processing techniques and

combination of both techniques. There are other techniques as well, but those are not necessary in connection to this thesis. Therefore, we will only emphasize statistical and signal processing techniques. The texture classification process involves two phases, the learning phase and the recognition phase. In the learning phase, the target is to build a model for the texture content of each texture class present in the training data, which generally comprises of images with known class labels. The texture content of the training images is captured with the chosen texture analysis method, which yields a set of textural features for each image. These features, which can be scalar numbers or discrete histograms or empirical distributions, characterize textural properties of the images, such as spatial structure, contrast, roughness, orientation, etc. In the recognition phase, the texture content of the unknown sample is first described with the same texture analysis method. Then the textural features of the sample are compared to those of the training images with a classification algorithm, and the sample is assigned to the category with the best match. In case, the best match does not meet the predefined criteria, the unknown sample can be rejected.

2.3 Statistical Analysis

Statistical methods analyze the spatial distribution of gray values by computing local features at each point in the image and deriving a set of statistics from the distributions of the local features. Depending on the number of pixels defining the local feature, statistical methods can be further classified into first-order, second-order and higher-order statistics. Some of the main statistical textural features are discussed in the following sections and detail can be found in [2].

2.3.1 First Order Statistical Features

Let *I* be the random variable representing the gray levels in the region of interest. The first order histogram *P(I)* is defined as:

$$P(I) = \frac{Number\ of\ \ pixels\ with\ gray\ level\ I}{Total\ number\ of\ \ pixels\ in\ the\ region}$$

Based on the above relation, the moments can be defined as:

$$m_i = \sum_{I=0}^{N-1} I^i P(I) \qquad i = 1,2,\cdots N-1 \tag{2.1}$$

where $m_0 = 1$ and m_1 is the mean value of I. Central Moments can be defined as:

$$m_i = \sum_{I=0}^{N-1} (I - m_1)^i P(I) \tag{2.2}$$

Most frequently used Central moments are Variance (μ_2), Skewness (μ_3) and Kurtosis (μ_4). Features from first order statistics provide information related to the gray level distribution of the image, but do not provide any information about the gray level distribution relative to their position.

2.3.2 Second Order Statistical Features

Spatial gray level co-occurrence estimates image properties related to second order statistics. Gray Level Co-occurrence Matrices (GLCM) have become one of the most well-known and widely used texture features. The *G x G* gray level matrix P_d for a displacement vector *'d'* and orientation *'?'* is defined as:

$$0\ degree : P(I(m,n) = I_1, I(m \pm d, n \pm d) = I_2)$$

$$= \frac{number\ of\ \ pairs\ of\ \ pixels\ at\ dist\ d\ \ with values\ (I_1, I_2)}{total\ number\ of\ \ possible\ \ pairs} \tag{2.3}$$

In a similar way:

45 degree : P(I(m,n) = I_1, I(m, n$\pm$ d) = I_2)

90 degree : P(I(m,n) = I_1, I(m $\pm$ d, n) = I_2) (2.4)

135 degree : P(I(m,n) = I_1, I(m $\pm$ d, n$\pm$ d) = I_2)

From each GLCM matrix, 14 different statistical measures can be extracted including angular second moment, contrast, correlation, variance, inverse difference moment, sum average, sum variance, sum entropy, difference variance, and difference entropy. Detailed discussion can also be found in [3], but some of the main feature measures are given below:

- *Angular Second Moment*

$$ASM = \sum_{i=0}^{G-1}\sum_{j=0}^{G-1} P(i,j)^2 \tag{2.5}$$

This feature is a measure of the smoothness.

- *Entropy*

$$ENT = \sum_{i=0}^{G-1}\sum_{j=0}^{G-1} P(i,j)\ \log P(i,j) \tag{2.6}$$

Entropy is a measure of randomness and takes low value for smooth images.

- *Contrast*

$$CON = \sum_{i=0}^{G-1}\sum_{j=0}^{G-1} (i-j)^2 P(i,j) \tag{2.7}$$

- *Inverse Difference Moment*

$$IDF = \sum_{i=0}^{G-1}\sum_{j=0}^{G-1} \frac{1}{1+(i-j)^2} P(i,j) \tag{2.8}$$

This feature takes high values for low contrast images due to the factor *(i-j)* in the denominator.

2.3.3 Autocorrelation Based Texture Features

The textural characteristic of an image depends on the spatial size of texture primitives. Large primitives give rise to coarse texture (e.g. rock surface) and small primitives give fine texture (e.g. silk surface). An autocorrelation function can be evaluated that measures this coarseness. This function evaluates the linear spatial relationships between primitives. If the primitives are large, the function decreases slowly with increasing distance, whereas it decreases rapidly if the texture consists of small primitives. However, if the primitives are periodic, then the autocorrelation increases and decreases periodically with distance. The set of autocorrelation coefficients given in (2.9) can be used as texture features [3].

$$C_{ff}(p,q) = \frac{MN}{(M-p)(N-q)} \frac{\sum_{i=1}^{M-p} \sum_{j=1}^{N-q} f(i,j) f(i+p, j+q)}{\sum_{i=1}^{M} \sum_{j=1}^{N} f^2(i,j)} \tag{2.9}$$

where p and q are the positional difference in the *'i'* and *'j'* direction respectively, and M and N are the image dimensions respectively.

2.3.4 Edge Frequency Based Texture Features

A number of edge detectors can be used to yield an edge image from an original image. We can compute an edge dependent texture description function E as follows:

$$\begin{aligned} E = &\left| f(i,j) - f(i+d, j) \right| + \left| f(i,j) - f(i-d, j) \right| + \\ &\left| f(i,j) - f(i, j+d) \right| + \left| f(i,j) - f(i, j-d) \right| \end{aligned} \tag{2.10}$$

This function is inversely related to auto-correlation function. Texture features can be evaluated by choosing specific distance d.

2.3.5 Primitive Length Texture Features

A gray level run is a set of consecutive pixels having the same gray level value. The length of the run is the number of pixels in the run [4]. Run length features encode textural information related to the number of times each gray level appears in the image by itself and number of times it appears in pairs and so on. Coarse textures are represented by a large number of neighboring pixels with the same gray level, whereas a small number represents fine texture. A primitive is a continuous set of maximum number of pixels in the same direction that have the same gray level. Each primitive is defined by its gray level, length and direction. If we were to represent *B(a, r)* as the number of primitives of all directions having length *'r'* and gray level *'a'*, then let *M*, *N* be image dimensions, *L* the number of gray levels, N_r the maximum primitive length in the images, and *K* the total number of runs given by:

$$GLRL = \sum_{a=1}^{L} \sum_{r=1}^{Nr} B(a, r) \tag{2.11}$$

The five features such as short primitive, long primitive, gray level uniformity, primitive length uniformity and primitive percentage can be defined by gray level run length matrix. Details can also be found in [3].

2.4 Texture Feature Extraction by Filtering

The most widely used techniques for textural feature extraction are statistical and signal processing. In the past, numerous algorithms were based upon the statistical analysis in which images can only be analyzed in the spatial domain. This problem was overcome by using transform techniques, and later on it was also proved by experiments on cats and apes visual system (similar to humans) that texture images can best be analyzed in the

filtered domain and multiresolution environment. Most of the recent techniques involve the use of multi-scale analysis in combination with statistical analysis for texture feature extraction. The main advantage of multiscale analysis is that they are capable of extracting even minute information, which may prove to be valuable for texture discrimination and classification. Multiscale approaches are mainly based upon multiple spatial domain filters, tuned Gabor filter and optimal filters etc.

2.4.1 Laws Filter Masks

A texture can be considered as a mixture of patterns. Therefore, characteristics of 'edges' and 'lines' are key elements to describe any texture. Even a plain or smooth texture can be considered as a texture without any edge. The early attempts to utilize spatial domain filtering as texture descriptors were emphasized on gradient (i.e. line and edge detector) filters such as Robert and Sobel operators [4]. Moreover, Laws proposed an effective filter based approach to texture analysis [5]. His approach consists of convolving images with a set of masks, which have been empirically designed to match primitive texture patterns. These masks are obtained by computing tensor products combined from several basic 1-D vectors. First, three basic vectors of length 3 are defined as:

$$L_3 = [1 \quad 2 \quad 1]$$

$$E_3 = [-1 \quad 0 \quad 1]$$

$$S_3 = [-1 \quad 2 \quad -1]$$

These are designed to measure the average gray level, edge and local peak (spot), respectively. 3 x 3 masks can be computed by forming outer products of any pair of

vectors, giving 9 different masks in total. By convolving the basic vectors with each other, a set of 5 distinct vectors of length 5 ($L_3 * S_3 = -E_3 * E_3$) are produced:

$$L_5 = L_3 * L_3 = [1 \quad 4 \quad 6 \quad 4 \quad 1]$$

$$E_5 = L_3 * E_3 = [-1 \quad -2 \quad 0 \quad 2 \quad 1]$$

$$S_5 = L_3 * S_3 = [-1 \quad 0 \quad 2 \quad 0 \quad -1]$$

$$W_5 = E_3 * S_3 = [1 \quad -2 \quad 0 \quad 2 \quad -1]$$

$$R_5 = S_3 * S_3 = [1 \quad -4 \quad 6 \quad -4 \quad 1]$$

By taking the outer products of these vectors, 25 masks of 5 x 5 can be generated. Various statistical attributes such as mean, energy, variance, kurtosis, skewness etc from convolved images can be treated as textural features. These statistics were used in classifying 944 texture images [6]. In another approach, Laws' masks were used and calculated the mean deviation of the convolved images as features for texture segmentation [7].

2.4.2 Fourier Domain Analysis

The Fourier transform and its fast version, FFT is a basic tool for harmonic analysis of images. The frequency analysis of the textured image is best done in the Fourier domain.

$$F(u,v) = \frac{1}{w^2} \sum_{x=1}^{M} \sum_{y=1}^{M} f(x,y) e^{\frac{-2pj}{w}(ux+vy)} \tag{2.12}$$

The human visual system analyzes the textured images by decomposing the image into its frequency and orientation components. Consider the image in the spatial domain *I(x,y)* and its Fourier transform *F(u,v)*, the quantity $|F(u,v)|$ is defined as the power spectra. Early approaches using such spectral features would divide the frequency domain region

into rings and wedges as given by (2.13) and shown in Figure 2.1 (a, b) [8]. Thus, total energy enclosed in the regions between rings and wedges can be treated as a useful feature. Regions can also be divided in horizontal and vertical strip regions and energy enclosed in the strips can be treated as a useful feature. Power spectral analysis may not yield robust textural features for classification due to poor time-frequency resolution property of Fourier analysis. Therefore, most of the researchers shifted to windowed Fourier transform and multiresolution environment in combination with Gabor filters [9, 10].

$$f_{r1,r2} = \int_{0}^{2p}\int_{r2}^{r1} |F(u,v)|\,dr\,dq \qquad f_{q1,q2} = \int_{q1}^{q2}\int_{0}^{\infty} |F(u,v)|^2\,dr\,dq \qquad (2.13)$$

where $r = \sqrt{u^2 + v^2}$ *and* $q = \tan^{-1}(v/u)$

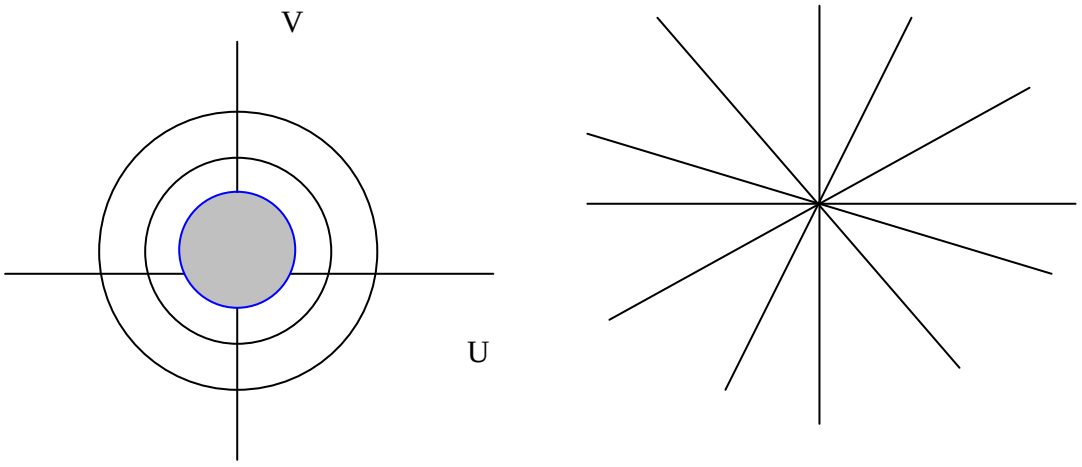

(a) Ring Division (b) Wedge Division

Figure 2.1 Frequency Domain Region Division

2.4.3 Gabor Filtering

More recently, Gabor filters, which constitute a particular class of windowed Fourier filters, have been used in image analysis. Typically, an image is filtered with a set of Gabor filters of different preferred orientations and spatial frequencies that cover appropriately the spatial frequency domain, and the features obtained form a feature vector field that is further used for analysis, classification, or segmentation. An input image $I(x,y)\ \ x,y \in \Omega$(x; y), (O the set of image points), is convolved with a two dimensional Gabor function $g(x,y)\ \ x,y \in \Omega$ consists of a sinusoidal plane wave of a certain frequency and orientation modulated by a Gaussian envelope. It is given by.

$$g(x,y) = e^{-\frac{(x'^2 + g^2 y'^2)}{2s^2}} \cos(2p\frac{x'}{l} + f) \qquad (2.14)$$

where $x' = x\cos q + y\sin q \qquad and \qquad y' = -x\sin q + y\cos q$

The standard deviation s of the Gaussian factor determines the effective size of the surrounding of a pixel in which weighted summation takes place. The eccentricity of the Gaussian and herewith the eccentricity of the convolution kernel g is determined by the parameter ?, called the spatial aspect ratio. The parameter ? is the wavelength and 1/? is the spatial frequency of the sinusoidal wave. Five spatial frequencies and four orientations were suggested and used and found that ? = 45^o is adequate [11].

In another design approach, one Gabor filter per texture was used [12]. The center frequency of each pre-filter was selected to correspond to a peak in the texture power spectrum and pre-filter bandwidths were determined by the center frequency. Limitation of a single filter for one or two texture images were somehow relaxed by the designing a single Gabor filter for the segmentation of multi-texture images [13].

In a different design approach, multi-channel Gabor filter in conjunction with competitive neural network can be optimized [14].

Type of "post-Gabor" processing in the above mentioned methods is different for feature extraction. It is interesting to evaluate the effect of the various types of nonlinear post-processing on the usefulness of the resulting features regarding texture discrimination and segmentation. Comparison of textural features based on Gabor filtering is given in [15], Gabor based energy, complex moment and grating cell operators were compared using the Fisher criterion and found out that grating cell operator gives the best discrimination and segmentation.

2.5 Filters and Filter Banks for Texture Analysis

Generally in the filtering and filter bank approach, measure of energy distribution, mean, variance etc. identifies and discriminates the texture image. Therefore, different statistical measures can be used for texture classification and discrimination if an image is decomposed into sufficient number of scales. At each scale, the filter bank acts as a band pass filter and the strength of corresponding frequency is estimated in each frequency bin. The spillover of energy in next bin is highly dependant upon the quality of frequency responses of filter banks.

Therefore, it is apparent that accurate segregation of frequency bins plays an important role in designing filters and filter banks. The design objective consists of their overall performance and performance of each individual filter. Table 2.1 summarizes various design objectives, which can be optimized for any particular application.

Table 2.1 Overall Design Objectives of Filter Banks

Filter	Design Objective
Overall filter bank	Minimize amplitude distortion
	Minimize aliasing distortion
	Minimize phase distortion
Single filter	Minimize stopband ripple
	Minimize passband ripple
	Minimize transition bandwidth
	Maximize passband flatness
	Maximize passband width

Figure 2.2 shows the two channel decomposition scheme where $H_k(z)$ and $G_k(z)$ are the pair of analysis and synthesis filters respectively.

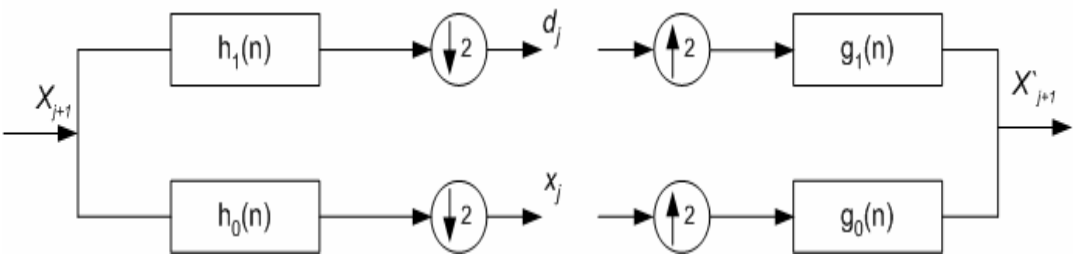

Figure 2.2 Two Channel Filter Bank

Practically, the analysis filters have non-zero transition bandwidth and stopband attenuation as shown in Figure 2.3. In case, the incoming signal is not band-limited, then its decimation would result in aliasing distortion. Ideally, the transition width of the two filters $H_o(e^{jw})$ and $H_1(e^{jw})$ should be narrow in such a way that there should be minimum overlap, but this would lead to expensive filters [16].

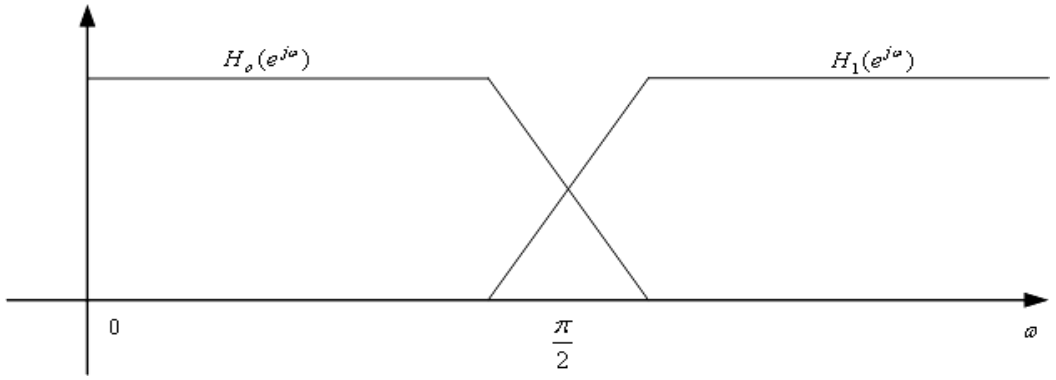

Figure 2.3 Magnitude Responses of Analysis Filters

Larger transition width and low stopband attenuation in analysis filters implies larger aliasing error. However, this distortion can be eliminated completely by careful choice of synthesis filters. In addition to aliasing distortion, phase distortion and amplitude distortion is also introduced by the analysis filters. Phase distortion can be eliminated completely by using linear phase filters, but amplitude distortion can only be eliminated by making overall system to be an all-pass which is practically impossible.

A comprehensive tutorial article on the theory and applications of multi-rate digital filters and filter banks can be found in [16, 17]. Several design methods of two channel perfect reconstruction (PR) filter banks with linear phase filters have been reported [18, 19]. A novel lattice structure design approach reports that good quality filters can be obtained by optimizing the lattice coefficients [20]. B.R. Horng *et al* proposed two new approaches for the design of two channel PR filter banks with linear phase filters. Both the approaches were based on the impulse response of the analysis filters. Unknown filter coefficients have been used as optimization parameters in Lagrangian quadratic programming problem with linear constraints. Similarly, several

researchers have used Lagrange multiplier approach for the design of PR filter banks [21-23].

Quadrature mirror filter bank (QMF) is another important class of filters, which incorporates both infinite impulse response (IIR) and finite impulse response (FIR) filters. The theory and applications of QMF filter banks are given in detail in [17]. Classical method for the design of QMF filter banks was proposed by Johnston, which incorporates minimization of stopband attenuation in objective function along with minimization of overall amplitude distortion as given by [24]:

$$|H(w)|^2 + \left|H(w - \frac{p}{M})\right|^2 = 1 \qquad for\ 0 < w < \frac{p}{M} \tag{2.15}$$

and $$|H(w)| = 0 \qquad for\ w > \frac{p}{M}$$

Creusere used the Parks McClellan algorithm for the design of filters which satisfy the (2.15) by varying the passband edges in the optimization process [25 - 27].

2.5.1 Optimal Filter Banks for Texture Discrimination

In general, methods adopted for filter bank design emphasize perfect reconstruction and good quality filters instead of catering to actual texture images to be discriminated. Thus, there is no guarantee that the filters banks would yield the required results for a specific set of texture images. Often, the solution to design problem ends up in lengthy filters, which are more expensive in terms of computation and time. In case of texture analysis, several features such as energy signatures, mean, variance, entropy etc are calculated on different decomposition levels. Therefore, synthesis filters can not play their part in

removing distortion effect. Hence, it is extremely important that transformed coefficients should be error free.

Design of an optimal QMF filter bank system based on max-flat polynomial for maximum possible texture discrimination is given in [28]. The main objective is to maximize texture discrimination along with attenuation of passband and stopband energies by placing sufficient number of zeros at $? = p$.

In another approach, a very simple, but effective optimization technique for maximum possible texture discrimination was proposed, which utilizes the Parks McClellan algorithm for the design of symmetric FIR filter. In an optimization process, filter order was fixed and passband and stopband edges were adjusted along with the relative error weighting factor. Symmetric impulse response filter with narrow transition width and reduced ripples in passband generally performs better as compared to an orthogonal filter with greater number of vanishing moments [29].

2.5.2 Filter Optimization for Texture Discrimination

In filter optimization, unknown filter coefficients are determined, which will maximize the distance between the local features obtained at the output of the filter using certain discriminant function. Several discriminatory functions are available, but few have been used in the past for texture analysis. A dissimilarity function based upon the ratio of their mean value is given as.

$$J_{MS} = \frac{m_{v1}}{m_{v2}} \tag{2.16}$$

A similar criterion was proposed, which deals more or less with the ratio of their means as well [31].

$$J_u = \frac{(m_{v1} - m_{v2})^2}{m_{v1} m_{v2}} \tag{2.17}$$

where m_{v1} and m_{v2} are the feature means. Both the above mentioned techniques deal only with the mean values, but do not cater for the variances of the coefficients.

Randen has optimized filters for two and more texture discrimination problems with respect to Fisher criterion which incorporates the variance along with their mean values in a dissimilarity measure [32, 33].

$$J_f = \frac{(m_{v1} - m_{v2})^2}{s_{v1}^2 + s_{v2}^2} \tag{2.18}$$

Where μ is the feature mean and s is the variance. A comparative study of filtering for texture classification can be found in [34] in which most of the major approaches such as Laws masks, ring/wedge filters, Gabor filters, wavelet transform, wavelet packets etc for texture feature extraction have been reviewed.

It has been concluded that various approaches yield different results for different images. Hence, none of the approaches can be treated as best for all kind of texture images. Therefore, there is a need for powerful texture measures and techniques, which can be used for robust texture classification with minimum complexity.

2.6 Summary

In this chapter, several techniques for texture image analysis and discrimination have been discussed and reviewed, which are primarily based on statistical and signal processing techniques. Furthermore, optimization techniques of filter and filter banks have also been discussed, but none of them proved to be a benchmark in the field of texture analysis and discrimination. The wavelet transform is another powerful tool that

has numerous applications in different fields. In the next chapter, the wavelet transform is discussed and its application to texture discrimination.

CHAPTER 3

MULTIRESOLUTION AND WAVELET BASED TEXTURE ANALYSIS

3.1 Introduction

In this chapter multiresolution and wavelet theory will be discussed along with its application in the field of texture analysis and discrimination. The working principle of multiresolution analysis techniques and the human visual system are more or less the same. Psycho-visual research provides the evidence that human beings process the images in a multi-scale way. Pre-processing of an image in the brain is similar to spatial frequency analysis and then different cells in the visual cortex respond accordingly to different frequencies. This phenomenon motivated the researchers to explore the application of multiresolution analysis to different areas.

3.2 Background of Multiresolution Analysis

Multiresolution techniques for signal and image processing have been in use for decades. There was a need of a transform that provides signal representation simultaneously in the spatial and frequency domain. In this context, various techniques were developed which, include Gabor, Haar, Walsh-Hadamard, filter banks etc. Solid and comprehensive theory of multiresolution was formulated in [35], which provides a framework for understanding and description of wavelet bases. The wavelet paradigm encompasses multiresolution decomposition of signal into orthogonal and biorthogonal wavelet functions which have

compact support and other properties. This technique enables precise decomposition of signal with little computational effort [36].

3.2.1 Time and Frequency Resolution

In any signal processing application, localization of a given basis functions in time and frequency domain is an important consideration. Signal domain methods require a high degree of localization in time, whereas frequency domain methods demand high degree of localization in frequency. This phenomenon would result in trade off between frequency and time localization. The definition of localization of a basis function is usually based on how it spans the area in the time-frequency plane.

Consider a signal $x(t)$ centered at t_o with its frequency spectrum $X(?)$ centered at $?_o$. The energy E of signal is given by two equations related by Parseval's theorem.

$$E = \int_{-\infty}^{\infty} |x(t)|^2 dt = \frac{1}{2p} \int_{-\infty}^{\infty} |X(w)|^2 dw \tag{3.1}$$

The values of t_o and $?_o$ are defined as centers of mass of the signal and its spectrum respectively.

$$t_o = \frac{1}{E} \int_{-\infty}^{\infty} |x(t)|^2 dt \qquad w_o = \frac{1}{E} \int_{-\infty}^{\infty} |X(w)|^2 dw \tag{3.2}$$

Time resolution width $?t$ of signal $x(t)$ can be defined by its root mean square:

$$\Delta t^2 = \frac{1}{E} \int_{-\infty}^{\infty} (t - t_o)^2 |x(t)|^2 dt \tag{3.3a}$$

similarly, for frequency resolution width ??.

$$\Delta w^2 = \frac{1}{2pE} \int_{-\infty}^{\infty} (w - w_o)^2 |X(w)|^2 dw \tag{3.3b}$$

3.2.2 Uncertainty Principle

The following uncertainty principle sets a bound on the maximum theoretical joint resolution in time and frequency represented by a product $\Delta t \Delta w$. If *x(t)* decays faster than $\frac{1}{\sqrt{t}}$ as $t \to \infty$, then uncertainty principle asserts:

$$\Delta t^2 \ \Delta w^2 \geq \frac{1}{2} \tag{3.4}$$

3.3 Multiresolution Analysis

A multiresolution analysis consists of a sequence of nested closed subspaces $V_j \subset L^2(R),\ j \in Z$.

$$\ldots \subset v_{-2} \subset v_{-1} \subset v_0 \subset v_1 \subset v_2 \ldots \tag{3.5}$$

$$v_j \subset v_{j+1}$$

Such that they possess the following properties:

- Upward and downward completeness $\bigcup_{j \in Z} V_j = L^2(R)$ and $\bigcap_{j \in Z} V_j = \{0\}$
- Scale invariance $f(t) \in V_j \Leftrightarrow f(2t) \in V_{j+1}$
- Shift invariance $f(t) \in V_o \Leftrightarrow f(t-k) \in V_o$

In addition to above mentioned properties, the final requirement for multiresolution concerns a basis for each space V_j. If a function *f (t)* is defined in V_o, then its orthonormal translates of *f (t-k)* would span the complete space and can be expressed as:

$$v_j = \overline{span_k \{f_{j,k}(t)\}} \tag{3.6}$$

A two dimensional family of functions is generated from the basic scaling function by translation and scaling.

$$f_{j,k}(t) = 2^{j/2} f(2^j t - k) \tag{3.7}$$

The nesting of spans of $f(2^j t - k)$ denoted by V_j in (3.5) is achieved by requiring $f(t) \in v_1$, which means that if $f(t)$ is in V_o, then it is also in V_1 space spanned by $f(2t)$. Hence, $f(t)$ can be expressed in terms of a weighted sum of shifted $f(2t)$ as:

$$f(t) = \sum_n h_0(n)\sqrt{2} f(2t - n) \tag{3.8}$$

Where $h(n)$ is a sequence of real numbers called the coefficients of a scaling function. Expression in (3.8) is also called dilation equation or multiresolution equation.

3.3.1 Wavelet Function

Important discriminant features of a signal can not be described efficiently by using the dilation equation. However, they can be described by defining a different set of function $y_{j,k}$, which spans the difference between the spaces. $y_{j,k}$ function is called the wavelet function.

$$y_{j,k}(t) = 2^{j/2} y(2^j t - k) \tag{3.9}$$

The scaling function $f(2^j t - k)$ are orthogonal at each scale V_j separately, but $f(t)$ is not orthogonal to $f(2t)$. Orthogonality across scales come from the wavelet subspaces w_j and their basis functions $y_{j,k}$. Orthogonality of scaling function and wavelet function allows simple calculation of expansion coefficients and Parseval's theorem that allows a partitioning of signal energy in the wavelet transform domain. The orthogonal

complement of v_j in v_{j+1} is defined as w_j, this means that all the members of v_j are orthogonal to all the members of w_j as given by

$$v_{j+1} = v_0 \oplus w_0 \oplus w_1 \oplus w_2 \ldots\ldots\ldots \oplus w_j \tag{3.10}$$

In general, the above equation can be written as:

$$L^2 = v_0 \oplus w_0 \oplus w_1 \oplus w_2 \ldots\ldots\ldots \oplus w_j \tag{3.11}$$

In practice, one can construct the spaces v_j and then take differences or construct the differences w_j and then take a sum. Since a wavelet resides in the space spanned by the next narrower scaling function, $w_0 \subset v_1$, it can be represented by a weighted sum of shifted scaling function $f_{j,k}(2t)$ with the different set of coefficients called wavelet coefficients as defined by

$$y(t) = \sum_n h_1(n)\sqrt{2} f(2t - n) \tag{3.12}$$

Where $h_0(n)$ and $h_1(n)$ are the coefficients of lowpass and highpass filters and in orthogonal wavelet system, they are related by expression

$$h_1(n) = (-1)^n h_0(1 - k). \tag{3.13}$$

Generally, coefficients $h_0(n)$ and $h_1(n)$ in (3.8) and (3.12) are computed in any design problem instead of dealing with scaling and wavelet function [37, 17].

3.3.2 Scaling and Wavelet Coefficients by Recursion

Initially, Mallat developed an efficient algorithm for computing decompositions and reconstructions of sampled signals, which is closely related to filter banks and have been in use for decades [35]. The multiresolution analysis framework on which orthonormal

and biorthogonal wavelet bases are constructed leads to efficient algorithm for computing wavelet coefficients. Relationships can be developed between the expansion coefficients at lower scales in terms of those at higher scales by using basic dilation equation (3.8) and are given in the following.

$$f(2^j t - k) = \sum_n h(n)\sqrt{2}\, f(2^{j+1} t - 2k - n) \tag{3.14a}$$

After changing variables $m = 2k+n$ the above equation becomes

$$f(2^j t - k) = \sum_m h(m - 2k)\sqrt{2}\, f(2^{j+1} t - m) \tag{3.14b}$$

A set of orthonormal basis function $f(t)$ and $y_{j,k}$ could span the complete space L^2 (**R**) and according to (3.11), any function $x(t) \in L^2$ (**R**) could be written as a series expansion in terms of scaling function and wavelet.

$$x(t) = \sum_k c_j(k)\, 2^{j/2} f(2^j t - k) \quad + \quad \sum_k d_j(k)\, 2^{j/2} y\,(2^j t - k) \tag{3.15}$$

Where $2^{j/2}$ maintain the unity norm of the basis function at various scales. $c_j(k)$ and $d_j(k)$ are the coefficients obtained at scale by taking the inner product.

$$c_j(k) = \left\langle x(t), f_{j,k}(t) \right\rangle = \int x(t) 2^{j/2} f(2^j t - k)\, dt \tag{3.16a}$$

re-arranging the above equation, we get

$$c_j(k) = \sum_m h(m - 2k) \int x(t) 2^{(j+1)/2} f(2^{j+1} t - m)\, dt$$

$$c_j(k) = \sum_m h_o(m - 2k)\, c_{j+1}(m) \tag{3.16b}$$

The corresponding relation for the wavelet coefficient is

$$d_j(k) = \sum_m h_1(m - 2k)\, c_{j+1}(m) \tag{3.17}$$

The implementation of (3.16) and (3.17) is illustrated in Figure 3.1.

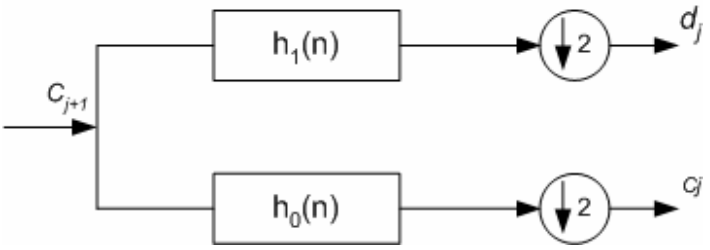

Figure 3.1 Analysis Bank

The signal approximation at some specific scale is expressed as in (3.15), which is a combination of approximation and detailing coefficients at next lower scale.

$$c_{j+1}(t) = c_j(t) + d_j(t) \tag{3.18}$$

Where $c_j(t)$ is the approximation signal and d_j is the detail at scale *"j"*. The overall complete representation of signal based upon approximation and detailing coefficients is expressed by (3.19).

$$x(t) = c_J(t) + \sum_{j=1}^{J} d_j(t) \tag{3.19}$$

where $c_J(t)$ is the approximation signal at the lowest scale and the next term is the summation of all the details. The signal can be reconstructed completely by the combination of averaging and detailing information at any stage.

3.4 Properties of Wavelet Bases

Bases functions are designed in a variety of ways. However, they are usually derived directly from multiresolution analysis. Important bases are local cosine bases, filter banks etc, but specialized bases are designed with respect to desired properties such as regularity, symmetry, finite support and orthogonal/ biorthogonal. These properties of wavelets serve as a key for selection of function for a specific application. Generally,

analysis of a signal needs non-orthogonal and compression requires orthogonal and smooth wavelet. Some important properties are discussed in this section for the construction of wavelet bases.

3.4.1 Compact Support

The compact support of a scaling and wavelet function can be defined as the closed interval in continuous time outside which the function is zero. Compact support of f and y is equivalent to having finite sequences and *h(z)* being a polynomial. Main reason for having smaller support is numerical efficiency and is directly proportional to wavelet recursion coefficients. For the existence of the solution of (3.8), scaling coefficients $h_o(n)$ must satisfy the following condition given by

$$\sum_n h_o(n) = \sqrt{2} \tag{3.20}$$

In frequency response, it is equivalent to requiring that FIR filter must have a response at DC equal to $\sqrt{2}$.

3.4.2 Symmetry

If the scaling function and wavelet are symmetric, then the filters have generalized linear phase. The absence of this property will lead to phase distortion.

3.4.3 Orthogonal Wavelet Bases

There are several advantages of scaling and wavelet function being orthogonal. Orthogonal bases function allows simple calculation of expansion coefficients and Parsavel's theorem relates the energy of a signal to the energy in each of the components

and their wavelet coefficients. Orthogonality of the scaling function *f(t)* can be related to its integer translates *f (t-k)* by following expression.

$$\int f(t)\, f(t-k) \;=\; d(k) \;=\begin{cases} E & if\ k=0 \\ 0 & otherwise \end{cases} \tag{3.21a}$$

Similarly, it can be written in terms of filter coefficients

$$\sum_n h(n)h(n-2k) \;=\; d(k) = \begin{cases} 1 & if\ k=0 \\ 0 & otherwise \end{cases} \tag{3.21b}$$

Orthogonality results in complicated design equations and prevents linear phase analysis. These problems can be eliminated by defining biorthogonal wavelet basis.

3.4.4 Biorthogonal Wavelet Bases

There are certain applications such as texture analysis, which requires symmetric wavelets. Symmetric wavelet basis can be constructed by defining dual set of scaling function, one for analysis and other for synthesis stage. Dual scaling function can be expressed as:

$$\begin{aligned} f(t) &= \sum_n h_0(n)\sqrt{2} f(2t-n) \\ \tilde{f}(t) &= \sum_n \tilde{h}_0(n)\sqrt{2} f(2t-n) \end{aligned} \tag{3.22}$$

For the existence of the solution of (3.8), dual set of filter coefficients $h_o(n)$ must satisfy the following relation.

$$\sum_n h_o(n) = \sum_n \tilde{h}_o(n) = \sqrt{2} \tag{3.23}$$

Similarly, a dual set of wavelet function can be defined as:

$$y(t) = \sum_n h_1(n)\sqrt{2}f(2t-n)$$
$$\tilde{y}(t) = \sum_n \tilde{h}_1(n)\sqrt{2}f(2t-n) \tag{3.24}$$

For perfect reconstruction and biorthogonality, it is required that dual scaling and wavelet coefficients must satisfy the following relationship.

$$\sum_k h_o(2k-m)\tilde{h}_o(2k-n) + h_1(2k-m)\tilde{h}_1(2k-n) = d(m-n) \tag{3.25}$$

Above equation can be simplified if $h_o(n), \tilde{h}_o(n), h_1(n), \tilde{h}_1(n)$ are related by [42]:

$$h_o(n) = (-1)^n \tilde{h}_1(n)$$
$$\tilde{h}_o(n) = (-1)^n h_1(n) \tag{3.26}$$

By substituting (3.26) in (3.25) we get

$$\sum_n \tilde{h}_o(n)h_o(n+2k) = d(k) \tag{3.27}$$

In case of orthogonality, $h_o(n)$ is orthogonal to even translations of itself, but for biorthogonality $\tilde{h}_o(n)$ is orthogonal to $h_o(n)$.

3.5 Comparison of Orthogonal and Biorthogonal Wavelets.

The biorthogonal wavelet system generalizes the orthogonal wavelet system and is more flexible and easy to design. Difference between them is summarized as below.

- The length of scaling and wavelet filter must be the equal and even, but this condition can be relaxed for biorthogonality.
- Symmetric wavelets and scaling function are possible in biorthogonal system. Linear phase filters are contrary to orthogonal filters.

- Parseval's theorem no longer holds for biorthogonal wavelet system i.e. the norm of coefficients is not the same as the norm of the function being spanned.
- Role of primary and dual filters can be switched easily in biorthogonal wavelet system.

3.6 Wavelet Based Image Analysis

In case of image analysis, wavelet transform can easily be extended to 2-D by using filtering approach. The wavelet transform of a 2-D image *I(x,y)* can be performed by applying the filters *H* and *L* sequentially along the rows and column of the image. The sub-images resulting from such an operator can be written as:

$$\begin{aligned} L^1(m,n) &= [L_x * [L_y * I]](x,y) \\ D_1^1(m,n) &= [L_x * [H_y * I]](x,y) \\ D_2^1(m,n) &= [H_x * [L_y * I]](x,y) \\ D_3^1(m,n) &= [H_x * [H_y * I]](x,y) \end{aligned} \tag{3.28}$$

Where * denotes the convolution operation, first convolution is performed along the columns of the image and the second operation is along the rows. L^1 is a smoothed version of an original image *I(x,y)* and D_1^1, D_2^1 *and* D_3^1 contains information of vertical, horizontal and diagonal directions respectively. The decomposition scheme is shown in Figure 3.2. By iterating the procedure on successive low pass images L^{i-1}, sub-images L^1, D_1^i, D_2^i *and* D_3^i on different levels are generated. This results in set of detail images for different scales. The frequency splitting of standard wavelet transform is in octave bands, which leads to an insufficient description of image, especially for higher frequencies.

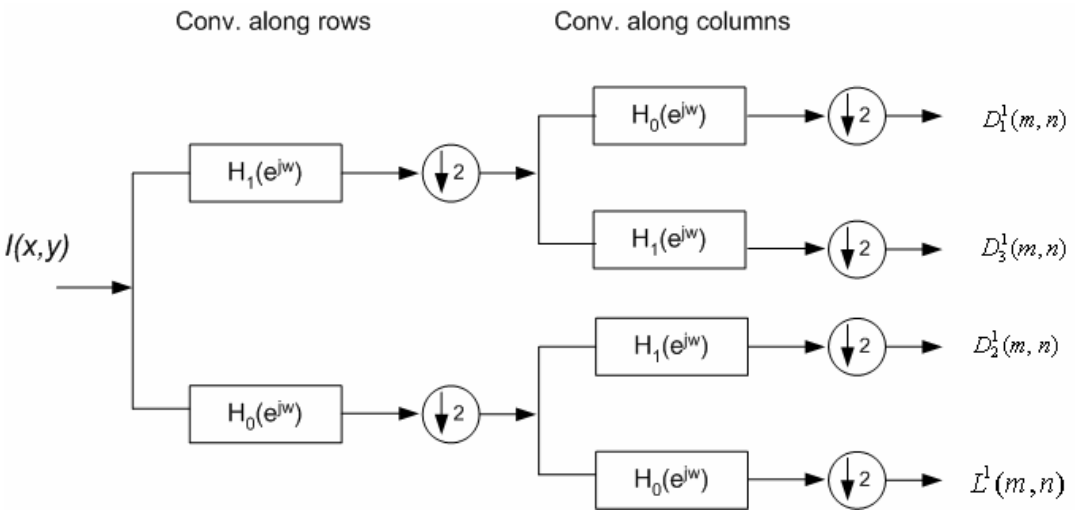

Figure 3.2 Wavelet Decomposition Scheme

This problem can be encountered by using wavelet packets, which refine the frequency splitting at the expense of larger number of sub-images resulting in higher computation [38, 39].

3.6.1 Wavelet Based Feature Extraction

The wavelet image decomposition provides a representation that is easy to interpret and every sub-image contains the information of a specific scale and orientation. For a *'d'* level decomposition, there are *3d+1* features for a standard decomposition and 4^d for a packet transform. Mean m , variance s and energy of detailing coefficients are few of the useful parameters, which can be used for texture classification and can be expressed as:

$$m = \frac{1}{MN}\sum_{m=1}^{M}\sum_{n=1}^{N} D_j^i(m,n)$$

$$s = \frac{1}{MN}\sum_{m=1}^{M}\sum_{n=1}^{N}[D_j^i(m,n) - m\ ]^2 \tag{3.29}$$

$$E_j^i = \frac{1}{MN}\sum_{m=1}^{M}\sum_{n=1}^{N}(D_j^i(m,n))^2$$

Where *M,N* are the dimensions of i^{th} sub-image and *j* denotes the decomposition level.

3.6.2 Wavelet Based Texture Analysis

Features are computed from sub-images of various scales and lead to a feature set, which reflects the scale properties of the texture. Energy features are mostly used in combination with other measures such as mean, variance, entropy etc. Tree structured wavelet transform is used to extract textural features. Each sub-image is repeatedly decomposed subject to some predefined threshold criteria on energies at different levels. Computed feature set based upon energies used for texture classification [39].

A different approach was employed by Unser for un-supervised segmentation of texture images in which he used local texture energy measures [40]. These measures were extracted using local linear transforms that have been optimized for maximal texture discrimination. Local statistics are estimated at the output of an equivalent filter bank by means of a non- linear transformation followed by an iterative Gaussian smoothing algorithm. A new feature reduction technique was applied to the data based on simultaneously diagonalzing scatter matrices evaluated at two different spatial resolutions. This new feature reduction method is an improvement on the commonly used Karhunen-Loeve transform and allows efficient texture segmentation based on simple thresholding.

In another approach, Unser developed redundant, shift invariant wavelet frames for feature extraction [41]. Channel variance was extracted as features using wavelet frames, which were used for segmentation and classification of texture images. The channel variances were estimated with the help of a sliding window on each sub-band, which yielded excellent classification results.

Xie and Brady applied wavelet frame decomposition to texture, and calculated local energy and phase as their texture features [47]. They developed a method which was based upon Hilbert transform to decouple the energy and phase component for their segmentation experiment. Laine and Fan investigated the use of energy and entropy measure from each wavelet packet and treated its real value as a distinct feature element. They suggested that such an analysis can provide a powerful method for accomplishing robust texture classification compared to traditional single resolution techniques [42].

Van de Wouwer used the discrete wavelet transform to extract the features for classification experiments. They used a combination of wavelet energy, mean deviation, histogram signatures and co-occurrence statistics for texture classification. Co-occurrence signatures yielded a lower classification error rate in comparison with the histogram signatures. However, best results were obtained by combining both the feature sets [43]. Classification of texture images, especially those with different orientation and scale change, is a challenging and important problem in image analysis and classification. Chi-Man and Lee propose an effective scheme for rotation and scale invariant texture classification using log-polar wavelet signatures [44]. The rotation and scale invariant feature extraction for a given image involves applying a log-polar transform to eliminate the rotation and scale effects. However, they at the same time produce a row shifted log-

polar image, which is then passed to an adaptive row shift invariant wavelet packet transform to eliminate the row shift effects. Therefore, the output wavelet coefficients become rotation and scale invariant. The adaptive row shift invariant wavelet packet transform is quite efficient with only *O(nlogn)* complexity. A feature vector of the most dominant log-polar wavelet energy signatures extracted from each sub-band of wavelet coefficients is constructed for rotation and scale invariant texture classification. A new rotation-invariant texture-analysis technique was proposed by Khouzani, which uses Radon and wavelet transforms. This technique utilizes the Radon transform to convert the rotation to translation and then applies a translation-invariant wavelet transform to the result to extract texture features. The proposed method is robust to additive white noise as a result of summing pixel values to generate projections in the Radon transform step. For evaluation purpose, several sets of textures along with different wave let bases were used and experimental results show the superiority of the proposed method and its robustness to additive white noise in comparison with some recent texture-analysis methods [45]. Guoliang Fan proposed wavelet-based texture analysis and synthesis using hidden Markov models HMM's. They developed a new HMM, called HMT-3S, for statistical texture characterization in the wavelet domain. In addition to the joint statistics captured by HMT, the new HMT-3S can also exploit the cross correlation across DWT sub-bands. The proposed HMT-3S is applied to texture analysis, including classification and segmentation, and texture synthesis with improved performance over HMT. Specifically, for texture classification, four wavelet-based methods, and experimental results show that HMT-3S provides the highest percentage of correct classification of over 95% upon a set of 55 Brodatz textures. For texture segmentation, it was demonstrated that more accurate

texture characterization from HMT-3S allows the significant improvements in terms of both classification accuracy and boundary localization[46].

Sebe and Lew investigated the problem of texture classification from a maximum likelihood perspective in which they considered the texture model, the noise distribution and the inter-dependence of the texture features. Their investigation showed that the real noise distribution is closer to an Exponential than a Gaussian distribution, and they also proposed the Cauchy metric as an alternative. Furthermore, they proposed a direct method for deriving an optimal distortion measure from the real noise distribution, which experimentally provides consistently improved results over the other metrics [47].

Mojsilovic investigated the application of non-separable wavelet transform for the texture characterization. They performed traditional dyadic wavelet decomposition and non-separable quincunx decomposition on a set of 21 Brodatz textures. In order to test their ability and classify textures in normal working conditions, noisy environment and with respect to rotation. Their experiments have shown that the quincunx transform is appropriate for characterization of noisy data, small number of resolution levels and shorter feature vectors and rotationally invariant description[48].

G. Lambert introduced an approach for multiscale wavelet based texture defect detection, in which specific problems were pointed out regarding localizing texture defects in multiscale wavelet representation. They also demonstrated the application of Trous algorithm on texture samples, which produced some better defect classification results [49].

Aleksandra studied the effect of wavelet properties (regularity, vanishing moments and shift invariance) for the selection of suitable bases for texture analysis and

characterization. It was found out that the selection of decomposition filter has a significant influence on the results of texture characterization. The optimal wavelet filter bank for texture analysis can be equated to the selection of FIR filters with good frequency localization and shorter impulse response [50].

3.7 Application Examples

Texture analysis is an important research area of machine vision. Potential areas of its application include biomedical image analysis, industrial inspection, analysis of satellite or aerial imagery, document analysis, material characterization etc. A brief survey of wavelet based texture analysis is given in next section.

3.7.1 Industrial Application

Stefan Livens presented a solution to two applications concerning the characterization of materials. The first application deals with the automatic characterization of surface corrosion images, which was handled using multiscale texture analysis approach. Second application dealt with the development of the automatic system for the characterization of silver halide micro-crystals in which the information regarding the shape, thickness and lateral size of the crystal was extracted [51].

Muid Mufti proposed an approach for feature extraction and failure classification that can be used for higher level control of complex systems. Algorithm/technique based upon fuzzy wavelet analysis was introduced which has the ability to extract the features from fuzzy data. The proposed technique was used for fabric fault detection and the

experimental data indicated the robustness and effectiveness of the proposed algorithm [52].

3.7.2 Medical Imaging

Aleksandra described a new approach for texture characterization based on non-separable wavelet decomposition and its application for the discrimination of visually similar diffuse diseases of liver. Classification experiments on a set of three different tissue types show that the scale/frequency approach, particularly one based on the non-separable wavelet transform could be a reliable method for a texture characterization and analysis of B-scan liver images. Comparison between the quincunx and the traditional wavelet decomposition suggests that the quincunx transform is more appropriate for characterization of noisy data and practical applications requiring description with lower rotational sensitivity [53].

In another application, Aleksandra proposed a new wavelet-based approach for analysis and classification of texture samples taken from very small areas of interest for the analysis of the myocardium or cancer recognition. The main idea of this method is to decompose the given image with a filter bank derived from an orthonormal wavelet basis and to form an image approximation with higher resolution. Texture energy measures calculated at each output of the filter bank as well as energies of synthesized images is used as texture features in a classification procedure. The method is tested with clinical data, and the classification results obtained are very promising. The performance of the new method is compared with the performance of several other transform-based methods.

The new algorithm has advantages in classification of small and noisy input samples, and it represents a step toward structural analysis of weak textures [54].

3.7.3 Remote Sensing

Remote sensing is a science of obtaining information about the attributes of the region without being in the close vicinity of the scene. Using various sensors mounted on aircrafts/satellite, data can be collected remotely that may be analyzed to extract useful information. There are several applications of texture analysis of remotely sensed images such as oceanography [55], soil classification [56, 57], ice classification [58, 59], crop analysis [60, 61], forest classification [62] etc.

3.8 Summary

The wavelet transform is a relatively recent mathematical development that has quickly found a place in many engineering applications. The mathematical basis of wavelet theory was presented in this chapter and its different properties, which may be critical in the construction of wavelets for specific application. In the later part of this chapter, survey of texture feature extraction based upon wavelet is discussed. Throughout the history of texture analysis, a large part of researchers' efforts have been spent on uncovering descriptive, compact features for textures. This has proved to be rather difficult, due mainly to the complex nature of textures. Early efforts have concentrated on pure statistical approaches, but neither has been fully satisfactory. In general, advancement in multiresolution signal decomposition has been found to be more suitable for textures analysis.

CHAPTER 4

DESIGN OF APPROPRIATE WAVELET BASES FOR TEXTURE DISCRIMINATION

4.1 Introduction

Texture analysis and discrimination is an active area of research in the field of computer vision. In this chapter, we propose a design of wavelet bases using genetic optimization, which will provide excellent discrimination between the multiple texture images. Our objective function is based on maximization of distinguishability measure involving the computation of finer details subject to some wavelet constraints. In contrast to well known orthogonal wavelet families, we have used extra degree of freedom in the design of the wavelet function for best possible texture discrimination. In the genetic optimization process, design parameters of the wavelet are optimized according to the characteristics of the texture images under a defined set of constraints.

4.2 Choice of Wavelet

Choice of wavelet for any particular application is still an open question. Some wavelet will be better suited for analyzing some specific set of texture images, yet they might not work for other set of images. Selection of appropriate wavelet bases function can be based upon the signal adaptive wavelet. Therefore, construction of an optimal set of wavelet function for a specific data set is commonly dealt in signal processing. Several methods have been developed in the past and discussed in the previous chapter for texture analysis and discrimination, but none of them converged to single solution due to

different underlying properties of texture images. Texture feature extraction at single scale or with the single filter may completely overlook the fine features as they are prevalent in intermediate scales.

Most commonly used are the Gabor wavelet filters for texture discrimination and analysis, but the problem associated with them is that central frequencies of the corresponding Gabor wavelet filters are tuned according to the frequencies corresponding to the principal spectral peaks of the texture. Therefore, the design of Gabor wavelet filters involves the investigation for the best frequencies and orientation of filters according to the characteristics of texture images. In case of multi-texture analysis, bank of Gabor filters are required to accomplish the task, which increases the computational complexity. In case of wavelet the transform, choice of suitable wavelet bases for texture discrimination is a critical issue. There are several factors involved in wavelet design, which can greatly affect the results such as regularity, length of wavelet, orthogonal or biorthogonal etc.

4.3 Design of Appropriate Wavelet Bases

We have proposed a scheme for the design of a wavelet bases for texture discrimination using genetic algorithm as presented by learning block diagram given in Figure 4.1. In the genetic optimization process, design parameters of wavelet are optimized according to the characteristics of the texture images under defined set of constraints. The designed wavelet maximizes the distinguishability function by moving the feature vectors of different textures apart with respect to a reference image, thus giving best possible texture

discrimination. Once the wavelet is designed for particular data set, it can be used for online feature extraction and classification as shown by the block diagram in Figure 4.2.

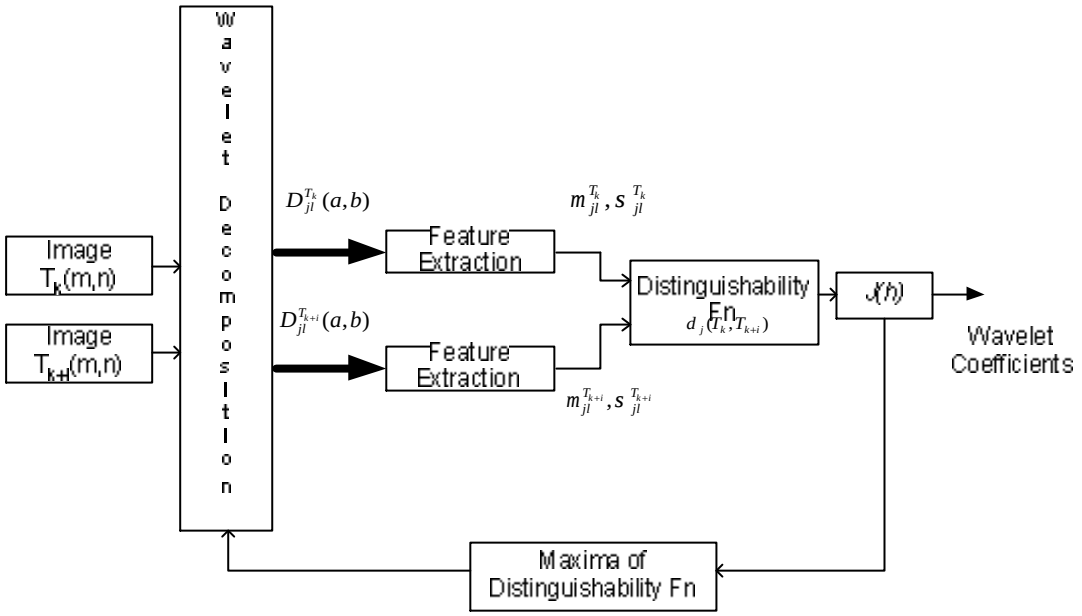

Figure 4.1 Learning System Block Diagram

In this technique, single mother wavelet function is required for a particular set of texture images which reduces the computational complexity. Experimental analysis has been carried out using remotely sensed texture images of Pakistan and wavelet function was optimized to illustrate the discrimination capability of the proposed technique. Classification results of optimized orthogonal/biorthogonal wavelet were compared with the existing wavelet families, which show that the results obtained are superior in terms of texture discrimination [63 - 65].

The wavelet transform represents the decomposition scheme of a signal into different resolution scales. Finer details of the signal can be analyzed at higher resolution

scales that are by reducing the width of the scaling function. These finer details play a significant role in signal analysis. In case of texture discrimination, difference in spaces spanned is more important and performance criteria should be to maximize the function involving the computation of finer details subject to some classical wavelet constraints.

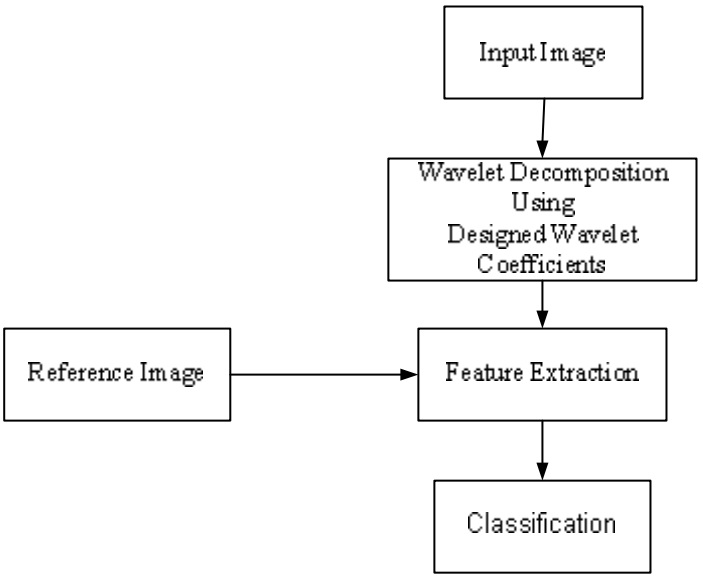

Figure 4.2 Online Classification System Block Diagram

The process of splitting a signal through pair of analysis filters and sub-sampling of signal by dropping every alternate sample is shown in a block diagram in Figure 4.3.

Let input signal be *x(n),* with Fourier transform $X(e^{jw})$is passed through the first analysis stage and expressions for Y_1 and D_1 after convolution and down sampling with analysis filters $H_f(e^{jw})$ and $H_y(e^{jw})$ are given as:

$$Y_1 = \frac{1}{2}\left[X(e^{jw/2})H_f(e^{jw/2}) + X(-e^{jw/2})H_f(-e^{jw/2}) \right]$$
$$D_1 = \frac{1}{2}\left[X(e^{jw/2})H_y(e^{jw/2}) + X(-e^{jw/2})H_y(-e^{jw/2}) \right] \quad (4.1)$$

Later terms in (4.1) with negative sign is a result of downsampling. In practice, the signal is bandlimited before passing through the downsampler.

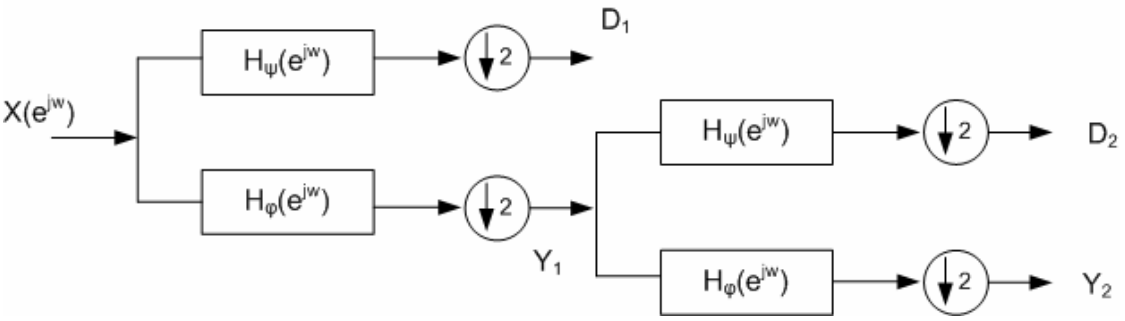

Figure 4.3 Two Stage Analysis Tree

Therefore, these negative terms are the non-overlapping replicas of the signal which has equal contribution. The expressions for Y_2 and D_2 after second level are given in a similar way:

$$Y_2 = \frac{1}{4}\begin{bmatrix} X(e^{jw/4})H_f(e^{jw/4})H_f(e^{jw/2}) \\ +X(-e^{jw/4})H_f(-e^{jw/4})H_f(-e^{jw/2}) \end{bmatrix}$$

$$D_2 = \frac{1}{4}\begin{bmatrix} X(e^{jw/4})H_f(e^{jw/4})H_y(e^{jw/2}) \\ +X(-e^{jw/4})H_f(-e^{jw/4})H_y(-e^{jw/2}) \end{bmatrix} \tag{4.2}$$

The generalized expression for D_j is given in (4.3), which are the detailing coefficients and carries information that plays an important part in discrimination of texture images.

$$D_j = \frac{1}{2^j}\begin{bmatrix} X(e^{\frac{jw}{2^j}})H_y(e^{jw/2})\prod_{k=1}^{j-1} H_f(e^{\frac{jw}{2^{k+1}}}) \\ +X(-e^{\frac{jw}{2^j}})H_y(-e^{jw/2})\prod_{k=1}^{j-1} H_f(-e^{\frac{jw}{2^{k+1}}}) \end{bmatrix} \tag{4.3}$$

As mentioned earlier in (3.13) that wavelet coefficients can be derived from the coefficients of scaling equation, therefore (4.3) can be modified and written as:

$$D_j = \frac{1}{2^j}\left[X(e^{\frac{jw}{2^j}}) \prod_{k=1}^{j} H_f(e^{\frac{jw}{2^k}}) + X(-e^{\frac{jw}{2^j}}) \prod_{k=1}^{j} H_f(-e^{\frac{jw}{2^k}}) \right] \tag{4.4}$$

Detailing coefficients D_j obtained at different scales can be used to extract information in order to form a feature vector.

4.3.1 Wavelet Decomposition of Image

A one dimensional wavelet transform can easily be extended for two dimensional signals. Set of texture images can be represented by 2-D function $T_k(m,n)$ $k = \{1 \cdots K\} \in \mathbf{N}$, serves as an input to the system, where $(m,n) \in \mathbf{N}$ are the spatial indices of images that vary from $m = \{1 \cdots M\} \in$ **N** and $n = \{1 \cdots N\} \in$ **N.** Simultaneously, pair of texture images under analysis are decomposed into wavelet decomposition coefficients $D_{jl}^{T_1}(a,b)$ and $D_{jl}^{T_2}(a,b)$ at different resolution levels using 2-D discrete wavelet transform given as:

$$\begin{aligned}
Y_j^{T_k}(a,b) &= \left[h_f * \left[h_f * Y_{j-1} \right] \downarrow 2,1 \right] \downarrow 1,2(a,b) \\
D_{j1}^{T_k}(a,b) &= \left[h_y * \left[h_f * Y_{j-1} \right] \downarrow 2,1 \right] \downarrow 1,2(a,b) \\
D_{j2}^{T_k}(a,b) &= \left[h_f * \left[h_y * Y_{j-1} \right] \downarrow 2,1 \right] \downarrow 1,2(a,b) \\
D_{j3}^{T_k}(a,b) &= \left[h_y * \left[h_y * Y_{j-1} \right] \downarrow 2,1 \right] \downarrow 1,2(a,b)
\end{aligned} \tag{4.5}$$

where:

$T_k(m,n)$ represents k^{th} texture image of MxN dimensions $(m,n,k) \in \mathbf{N}$

$Y_j^{T_k}(a,b)$ represents low resolution image of k^{th} original image at j^{th} resolution level.

$D_{jl}^{T_k}(a,b)$ represents detail image coefficients of k^{th} original image at j^{th} resolution level.

* represents convolution operator

$\downarrow 2,1$ sub-sampling along rows and $\downarrow 1,2$ sub-sampling along columns

h_f scaling filter coefficients and h_y wavelet filter coefficients

l=1,2 and 3 represents vertical, horizontal and diagonal coefficients respectively.

Thus after wavelet decomposition, original texture image $T_k(m,n)$ can be represented by set of sub-images $\{ Y_j^{T_k}(a,b) and \ D_{jl}^{T_k}(a,b) \}_{(j=1...J) \ and \ (l=1,2,3)}$, which is a multi-scale representation of original image. Each set of wavelet coefficients contains unique information of the texture image, which can be used to form a feature vector.

4.3.2 Feature Extraction

Wavelet coefficients $D_{jl}^{T_k}(a,b)$ obtained at different resolution levels contain important information from discrimination point of view. Mean $m_{jl}^{T_k}$ and variance $s_{jl}^{T_k}$ of the wavelet detail coefficients at different scales can be used to form a feature vector, which illustrates the distribution of texture attributes.

$$m_{jl}^{T_k} = \frac{1}{AB} \sum_a \sum_b D_{jl}^{T_k}(a,b) \tag{4.6}$$

$$s_{jl}^{T_k} = \frac{1}{AB} \sum_a \sum_b [D_{jl}^{T_k}(a,b) - m_{jl}^{T_k}]^2$$

Where $m_{jl}^{T_k}$ is the mean value of coefficients of k^{th} image at j^{th} level. Similarly, $s_{jl}^{T_k}$ is the variance of coefficients of k^{th} image at j^{th} level for *{l=1,2,3}* and A and B are the dimensions of image.

4.3.3 Distinguishability Measure

The system shown in Figure 4.1 compares two texture images under analysis at a time and computes their features $m_{jl}^{T_k}$ and $s_{jl}^{T_k}$ at different scales. These computed features can be used to find the discrimination between two texture images. We have used Fisher discrimination measure (4.7) in our optimization routine, because maximization of difference of means would move the feature vectors apart and reduction in variance would help in eliminating the chance of texture classes getting intermingled.

$$f_{jl}(T_k, T_i) = \frac{(m_{jl}^{T_k} - m_{jl}^{T_i})^2}{(s_{jl}^{T_1})^2 + (s_{jl}^{T_2})^2} \tag{4.7}$$

Where $f_{jl}(T_k, T_i)$ is the discriminant value of the function between the two textured images T_k and T_i at j^{th} level for *{l=1,2,3}*. In a multiresolution environment, discriminant values obtained by (4.7) at each scale can be combined by defining another function called the distinguishability function:

$$d\ (T_k, T_i) = \sum_j \left[f_{j1}(T_k, T_i) + f_{j2}(T_k, T_i) + f_{j3}(T_k, T_i) \right] \tag{4.8}$$

Distinguishability function $d\ (T_k, T_i)$ is a combined measure of discrimination between the two textured images T_k and T_i *{i=1…k}* at all the resolution levels. Practically, auto-distinguishability measure *(i =k)* should be zero and co-distinguishability measure $(i \neq k)$ should have finite value ß.

$$d\ (T_k, T_i) = \begin{cases} 0 & for\ i = k \\ b & i \neq k \end{cases} \tag{4.9}$$

Wavelet bases designed by optimizing the distinguishability function are highly dependant upon the attributes of textured images and maximize the distance between the

features in best possible manner. Distinguishability function $d\ (T_k, T_i)$ would attain less value of ß in (4.9) for images having similar properties and vice versa. In general, real world images are a combination of different regions exhibiting textural properties. Therefore, an overall objective function is needed to be defined which computes distinguishability measure of reference image with every other image present in the natural scene. An overall objective function can be defined as:

$$J(h_j) = \max_{(h_j)} \sum_{i=1}^{I} \sum_{k=1}^{K} d(T_k, T_i) \tag{4.10}$$

Given a set of texture images $T_k(m,n) \quad k = \{1 \cdots K\} \in \mathbf{N}$ from a natural scene, objective is to search a set of scaling filter coefficients h_f, which will maximize the function *J(h)* given in (4.10) under a set of constraints given in the following section.

4.4 Necessary Conditions for Wavelet Design

There are certain necessary and sufficient conditions which are required for the design of wavelet bases. These conditions are discussed in next section.

4.4.1 Convergence of Product Series

The product term involved in (4.4), $\prod_k H_f(e^{jw/2^k})$ can be used theoretically to prove the existence of scaling function and also calculating its coefficients. A minimum requirement for the convergence of this or any product series is that the factor $H_f(e^{jw/2^k})$ must approach to one as $k \to \infty$, therefore $H_f(0) = 1$, which means $h_f(n)$ must be a low pass filter with zero at z = -1.

4.4.2 Compact Support

For the existence of the solution of (3.8), scaling coefficients $h_f(n)$ must satisfy the following condition given by

$$\sum_n h_f(n) = \sqrt{2} \tag{4.11}$$

In frequency response, it is equivalent to requiring that FIR filter must have a response at DC equal to $\sqrt{2}$.

4.4.3 Orthogonality

In our design problem, we require that the scaling function should be orthogonal to its integer translates as given by

$$\begin{aligned} \sum_n h_f(n) h_f(n-2k) = d(k) = 1 \qquad & for \quad k = 0 \\ = 0 \qquad & otherwise \end{aligned} \tag{4.12}$$

4.4.4 Biorthogonal Wavelet Expansion

An orthogonal wavelet system across both translations and scaling gives a clean, robust and symmetric formulation with the Parseval's theorem. It relates the energy of the signal to the energy distributed in each of the components and their wavelet coefficients. Conditions for an orthogonal system require greater degree of freedom, which results in complicated design equations. Moreover, orthogonal and symmetric filters can not be designed at the same time due to the distribution of zero's of a polynomial. Therefore, a switchover to biorthogonal wavelet system allows linear phase system and they are much easier to design. In orthogonal wavelet systems, analysis filters (h_f, h_y) and synthesis

filters (g_f, g_y) shown in Figure 4.4 are time reversal of each other and are given in (3.13).

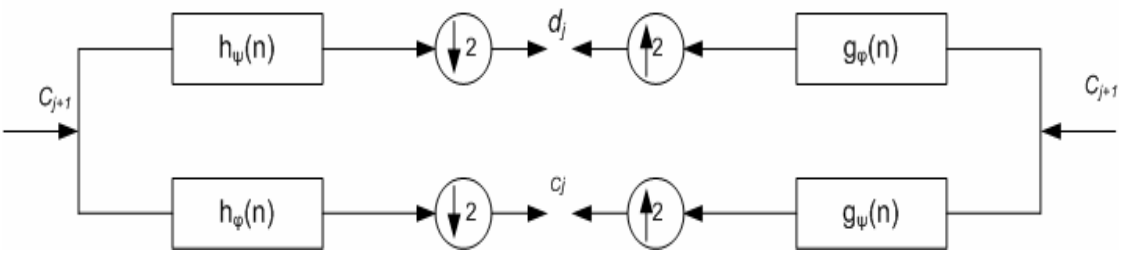

Figure 4.4 Wavelet Analysis and Synthesis Scheme

In case of biorthogonal, the condition of orthogonality can be relaxed and they are related by expression given in (4.13). For perfect reconstruction, analysis and synthesis filters have to satisfy the following relation:

$$\sum_k h_j(2k-m)g_y(2k-n) + g_j(2k-m)h_y(2k-n) = d(m-n) \tag{4.13}$$

The above equation can be simplified if the analysis and synthesis filters are related by:

$$h_y(n) = (-1)^n g_y(1-n)$$

and (4.14)

$$g_j(n) = (-1)^n h_j(1-n)$$

These four filters are cross related by time reversal and flipping signs of every other element. Substituting (4.14) into (4.13), we obtain:

$$\sum_n h_f(n)g_y(2k+n) = d(k) \tag{4.15}$$

Here $h_f(n)$ is orthogonal to $g_f(n)$, which gives the name biorthogonal.

4.4.5 Regularity

Regularity is defined in terms of zeros of the transfer function or frequency response of an FIR filter made up from the scaling coefficients. This is related to the decay of magnitude of Fourier transform as frequency goes to infinity. A scaling filter is said to be K regular if its Z-transform has K zeros at z= -1. Transfer function of scaling filter can be expressed as.

$$H_f(z) = \left(\frac{1+z^{-1}}{2} \right)^K Q(z) \tag{4.15}$$

where $H_f(z)$ is the z-transform of the scaling coefficients and $Q(z)$ has no zeros at location z = -1. Daubechies used maximum regularity in order to obtain maximum smoothness of scaling function, but this condition can be relaxed in order to achieve other design purposes. In time domain, scaling filter is K regular if it satisfies the following relation.

$$\sum_n n^k (-1)^n h_f(n) = 0 \qquad for\ k = 0,1,2,3...K-1 \tag{4.16}$$

4.5 Offline Learning Using Genetic Algorithms

Genetic Algorithms (GA's) are adaptive heuristic search algorithm based on the evolutionary ideas of natural selection and genetics [66]. As such they represent an intelligent exploitation of a random search used to solve optimization problems. Although randomized, GA's are by no means random, instead they exploit historical information to direct the search into the region of better performance within the search space. The basic techniques of the GA's are designed to simulate processes in natural systems necessary for evolution. It follows the principles first laid down by Charles Darwin of "survival of

the fittest.", that is competition among individuals results in the fittest individuals dominating over the weaker ones. GA's simulate the survival of the fittest among individuals over consecutive generation for solving a problem. Each generation consists of a population of character strings that are analogous to the chromosome that we see in our DNA. Each individual represents a point in a search space and a possible solution. The individuals in the population are then made to go through a process of evolution. GA's are based on an analogy with the genetic structure and behavior of chromosomes within a population of individuals. Individuals in a population compete for resources and mates, those individuals most successful in each 'competition' will produce more offspring's than those individuals that perform poorly. Genes from `good' individuals propagate throughout the population, so that two good parents will sometimes produce offspring that are better than either parent. Thus each successive generation will become more suited to their environment.

4.5.1 Key Terms Used in Genetic Algorithms

Based upon natural selection, after an initial population is randomly generated (unknown variables), GA evolves through three operations.

4.5.1.1 Selection Operation

The key idea in the selection procedure is to give preference to better individuals, allowing them to pass on their genes to the next generation. The goodness of each individual depends on its fitness. Fitness may be determined by an objective function or by a subjective judgment.

4.5.1.2 Crossover Operation

Two individuals are chosen from the population using the selection operator and a crossover site along the bit strings is randomly chosenas shown in Figure 4.5. The values of the two strings are exchanged up to this point, if S1=000000 and S2=111111 and the crossover point is 2 then S1'=110000 and S2'=001111. The two new offspring created from this mating are put into the next generation of the population by recombining portions of good individuals. This process is likely to create even better individuals.

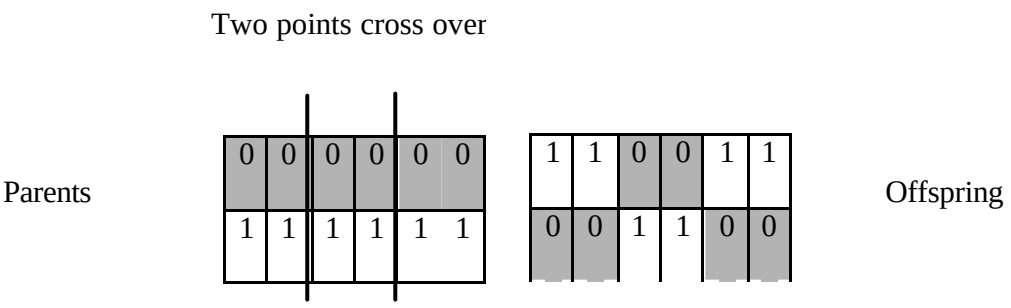

Figure 4.5 Two Point Crossover Method

4.5.1.3 Mutation Operation

The portion of the new individuals will have some of their bits flipped with low mutation rate, purpose is to maintain diversity within the population and inhibit premature convergence. Mutation and selection (without crossover) create a parallel, noise-tolerant, hill-climbing algorithm.

4.6 Solving for Appropriate Wavelet Using Genetic Algorithm

The aim of the design problem is to search for unknown scaling filter coefficients h_f, that will maximize the objective function given in (4.10) subject to constraints in (4.11),

(4.12) and (4.16). The normalization constraint on $h_f(l)$ can easily be implemented in the frequency domain by implementing conditions of ideal low pass and high pass filter. If stopband and passband frequencies can be denoted by w_s and w_p, then stopband energy E_s with cutoff frequency w_s can be defined as:

$$E_s = \int_{w_s}^{p} \left[H_f(w)\right]^2 dw + \int_{0}^{wp} \left[H_y(w)\right]^2 dw \tag{4.17}$$

Passband energy E_p with cutoff frequency w_p can be defined as:

$$E_p = \int_{0}^{w_p} \left[H_f(w) - 1\right]^2 dw + \int_{w_s}^{p} \left[H_y(w) - 1\right]^2 dw \tag{4.18}$$

The overall constrained optimization problem can be restated for genetic optimization by

$$Fitness\ \ function = \min_{(h_f)} \left\{ - J(h_f) \right\} \tag{4.19}$$

subject to constraints given by (4.11), (4.12), (4.17) and (4.18). Unknown individuals (variables) are the h_f coefficients of scaling function.

4.7 Summary

In this chapter, we have developed a performance metric based upon a differentiability function. It does not only maximize the difference between the mean values of the detailing coefficients of texture images obtained at different resolution levels, but also reduces the variances. Reduction in variance cloud would further apart the classes of different textures, which would make the classification more robust. Double summation in objective function (4.10) includes all the texture images in the database or templates of textures generated from a single satellite/aerial image. We have also discussed the necessary and sufficient constraints for the design of image/signal adaptive wavelet.

CHAPTER 5

RESULTS OF DESIGNED WAVELET FOR TEXTURE DISCRIMINATION

5.1 Introduction

In the previous chapter, we have developed a technique for the design of appropriate wavelet for best possible texture discrimination by maximizing the objective function given in (4.10) under set of constraints given in Section 4.4. The proposed technique is flexible in such a way that it can be applied to any particular set of texture images. In this research work, templates of texture images extracted from a complex natural satellite/aerial image serves as an input to the system for the design of appropriate wavelet. We have designed two different types of wavelets orthogonal and biorthogonal by using same set of texture images in a genetic optimization process. Results of designed wavelet are given in comparison with other well known wavelet families to illustrate the effectiveness of the proposed technique [65].

5.2 Simulation Data Used in the Design Process

We have analyzed different regions of Pakistan based upon textural characteristics by using samples of satellite images as shown in Figure 5.1. Samples of dimension 2000 x 2000 were acquired by using Google earth at an altitude of 50,000 feet. Terrain of Pakistan can roughly be divided into five classes.

Class 1: Cultivated land: Samples of texture images shown in Figure 5.1(a) can be classified as the cultivated land along the river Indus. Three samples were acquired from

different locations 32° 03`N & 73° 21` E, 31° 19`N & 73° 34` E and 31° 11`N & 73° 34` E respectively.

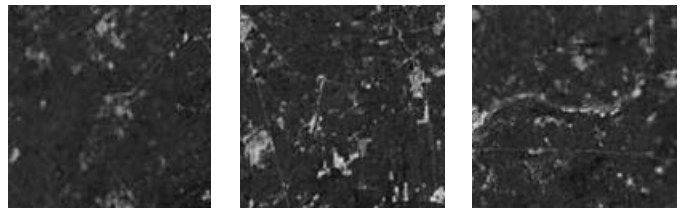

(a) Cultivated Land

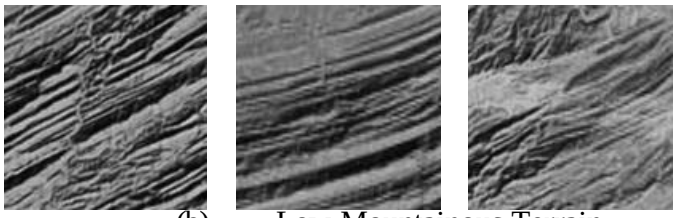

(b) Low Mountainous Terrain

(c) Desert Area

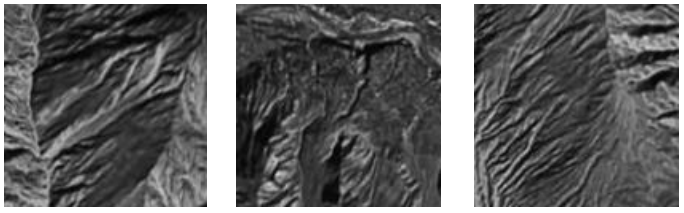

(d) Higher Mountains (Himalayas)

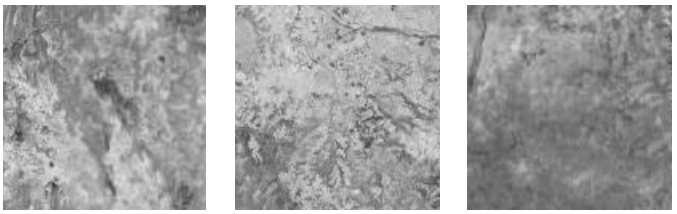

(e) Potohar Plateau

Figure 5.1 Five Classes of Texture Images Obtained from Google Earth

Class 2: Low mountainous terrain: Samples of texture images shown in Figure 5.1(b) can be classified Low mountainous terrain in Balochistan province. Three samples were acquired from different locations 31^{o} 15`N & $68^{o}$ 21` E, 30^{o} 59`N & $68^{o}$ 12` E and 27^{o} 26`N & $64^{o}$ 39` E respectively

Class 3: Desert area: Samples of texture images shown in Figure 5.1(c) can be classified as desert area scattered in south of Pakistan. Three samples were acquired from different locations 28^{o} 35`N & $71^{o}$ 42` E, 28^{o} 36`N & $71^{o}$ 39` E and 25^{o} 27`N & $67^{o}$ 52` E respectively.

Class 4: Higher mountains: Samples of texture images shown in Figure 5.1(d) can be classified as high mountains Himalayas range in extreme north of Pakistan. Three samples were acquired from different locations 36^{o} 24`N & $74^{o}$ 29` E, 36^{o} 19`N & $74^{o}$ 13` E and 36^{o} 17`N & $73^{o}$ 55` E respectively.

Class 5: Plateau: Samples of texture images shown in Figure 5.1(e) can be classified as a plateau. Three samples were acquired from different locations of Potohar plateau 33^{o} 20`N & $72^{o}$ 41` E, 33^{o} 16`N & $73^{o}$ 06` E and 33^{o} 24`N & $73^{o}$ 04` E respectively.

Suitable wavelet was designed by using all the texture images shown in Figure 5.1 by maximizing the objective function given in (4.10) with reference to texture image of cultivated land.

5.3 Parameters Used in Genetic Optimization During Offline Learning

We have used Genetic Algorithm toolbox available in MATLAB 7.1 environment for the design of the desired wavelet. Simulations time of 115 minutes was recorded during

offline learning on Pentium IV machine (2.8 GHz and 256MB Ram). Following are the parameters set for the optimization routine:

$$Fitness\ function \quad F = \min_{(h_f)} \{ -J(h_f) \}$$

$$Unknown\ variables \Rightarrow h_f(n) \qquad for\ n = 1 \cdots N$$

Population size = 20

Number of maximum generations = 1000

Stall generation (number of generations in which fitness value is unchanged) = 50

Two point crossover

Mutation rate 0.01

We have used the same set of parameters for orthogonal and biorthogonal wavelet design. Results and performance of both the designed wavelets are presented in the following sections.

5.4 Results of Appropriate Orthogonal Wavelet Design

In this design problem, we have optimized the wavelet for two different lengths of scaling coefficients (N=4,6). Same set of texture images were used in the design process to highlight the effect of increased length of wavelet on texture discrimination. In case of lengths lower than four as in case of Haar wavelet, it does not allow any degree of freedom to search for the maxima of the objective function. Similarly, by increasing the length of the wavelet filter coefficients, computationally complexity will also increase. The objective is to search for unknown scaling filter coefficients, which will maximize the objective function expressed by (4.19). Necessary and sufficient constraints were incorporated in the design of appropriate wavelet. As mentioned earlier, the scaling filter

should be a low pass filter and must have at least one zero at ? = p for the convergence of the product series. Therefore, we used the extra degree of freedom (zeros at ? = p) in search of maxima of objective function. Figure 5.2 shows the fitness function value for 1000 generations, which finally converged to the value of 8.162 for orthogonal wavelet design.

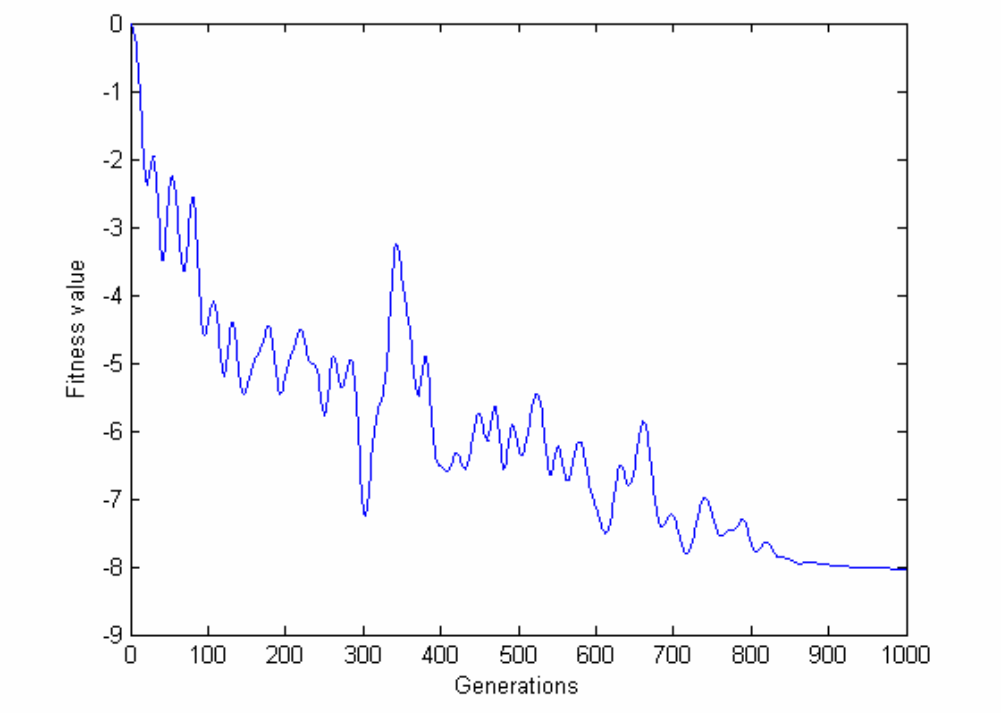

Figure 5.2 Convergence of Genetic Algorithm

Shape of the scaling function f_0 generated by the proposed scaling function is less smooth as compared to Daubechies scaling function f_d shown in Figure 5.3(a)and (b). In fact, Daubechies has used maximum number of zeros at ? = p for smoother wavelet.

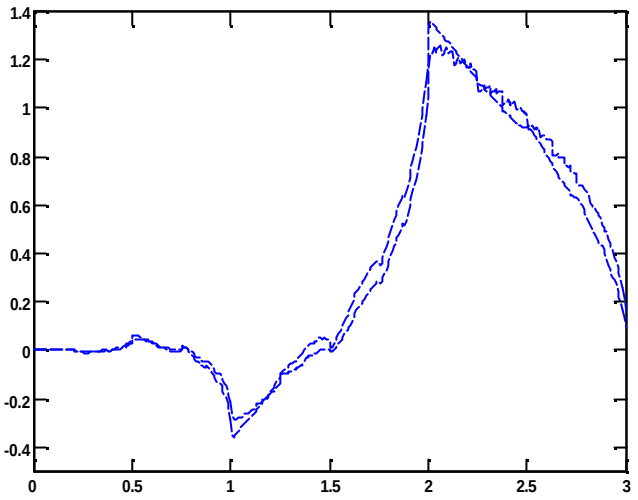

(a) Length N = 4

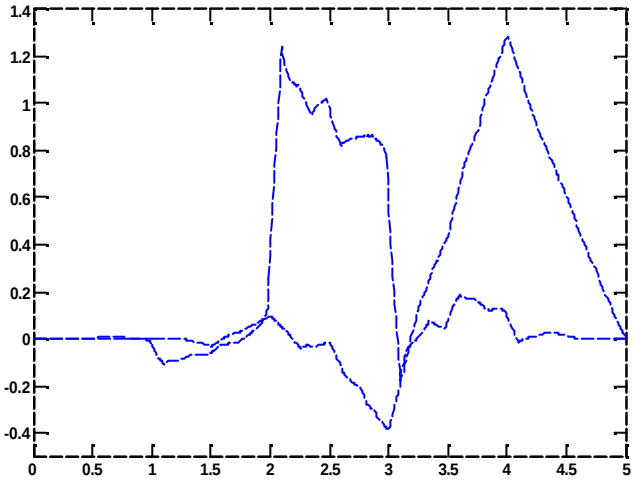

(b) Length N = 6

Figure 5.3 Responses of Appropriate F_o (solid) and Daubechies Scaling Function f_d (dotted)

Table 5.1 shows the results of objective function *J(h)* of appropriate wavelets for two different lengths in comparison with different orthogonal and biorthogonal wavelet families. It can be observed from the results that increase in length of scaling function

F(t) does not help in achieving more discrimination between texture images. Increase in length would also become more demanding in terms of computation and processing time.

Table 5.1 Results of *J(h)* for Appropriate and Different Wavelet Families

Wavelet Family	*J(h)*	Wavelet family	*J(h)*	Wavelet family	*J(h)*	Wavelet family	*J(h)*
App. wavelet (N=4)	**8.162**	db2	0.07	Sym2	0.70	Bior2.2	0.12
		db4	0.15	Sym8	0.12	Bior4.4	0.06
App. wavelet (N=6)	**5.49**	db6	0.27	Coif2	0.10	Bior6.8	0.16
		db10	0.30	Coif4	0.22	Rbior4.4	0.07

Therefore, it can be concluded from the results that App. wavelet of length (N=4) is best suited amongst other wavelets for given set of texture images. Frequency response of scaling function and scaling filter is shown in Figure 5.4(a) and (b) in comparison to Daubechies filters. Proposed filter has got wider transition bandwidth as compared to Daubechies but we have achieved higher discrimination capability. Proposed filter coefficients are given in Table 5.2.

Table 5.2 Scaling Filter Coefficients of Appropriate Wavelets

N	0	1	2	3	4	5
App. wavelet N=4	-0.1198	0.1875	0.8214	0.5252	-	-
App. wavelet N=6	-0.061	0.050	0.800	0.551	-0.05	0.110

Distinguishability function expressed by (4.8) maximizes the difference between two texture images. Therefore, we kept the texture image of cultivated region Figure 5.1(a) as reference and used rest of the images to calculate the difference between the feature vectors.

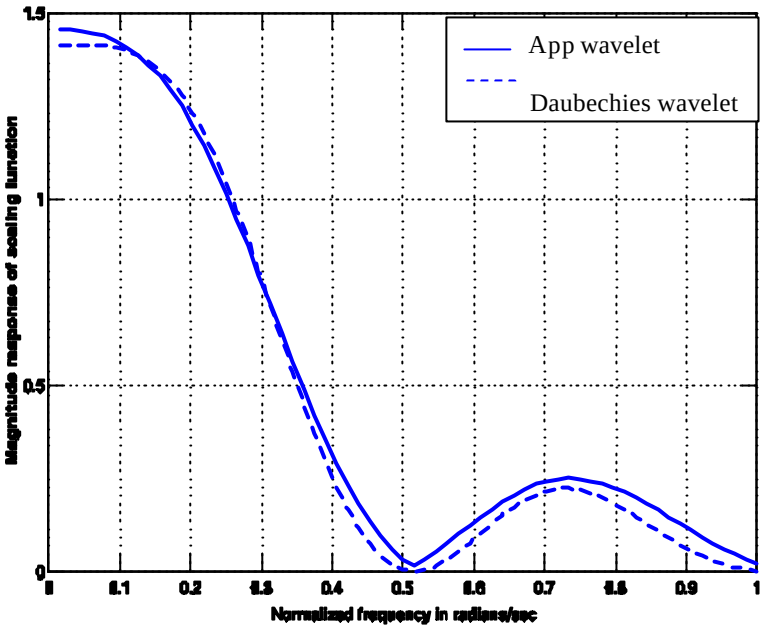

(a) Frequency Response of Scaling Function

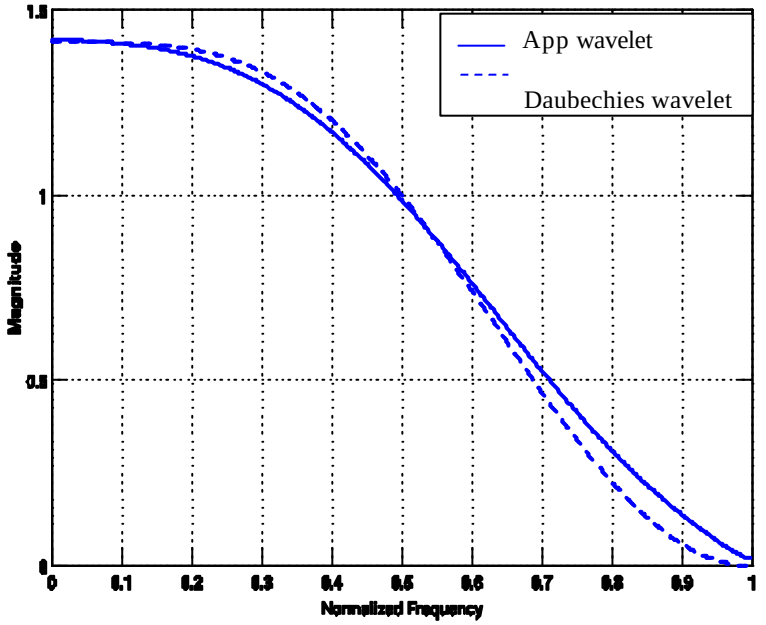

(b) Frequency Response of Scaling Filter

Figure 5.4 Responses of Appropriate (N=4) (solid) and Daubechies Scaling Function (dotted)

Results of Distinguishability function up to three decomposition levels are listed in ascending order with reference image as given in Table 5.3. Comparison of proposed wavelet with other well known orthogonal and biorthogonal wavelet families such as Daubechies, Symlet and Coiflet shows that the results obtained by appropriate wavelet with length N=4 is superior in terms of distinguishability. Moreover, the proposed wavelet of length four out performs even Daubechies wavelet of length N =10. Therefore, in order to save computational complexity, we did not extend our design further to higher lengths of scaling coefficients. Well known wavelet families have hardly shown any distinguishability amongst different regions. On the other hand, proposed wavelet has shown great deal of discrimination between different regions.

Table 5.3 Performance Comparison of Distinguishability Function $d(T_g, T_i)$ for Different Texture Images in Comparison with Texture Image of Cultivated Region

Class type	Samples	**App.4**	**App.6**	db2	db4	sym2	sym8	coif4	bi2.2
Cultivated region	I	**0**	**0**	0	0	0	0	0	0
	II	**0**	**0.001**	0	0	0.018	0	0.005	0.001
	III	**0**	**0.001**	0.008	0.006	0.002	0.003	0	0.001
Low mountain	I	**0.158**	**0.211**	0.045	0.035	0.010	0.011	0.004	0
	II	**0.292**	**0.161**	0.032	0.057	0.072	0.023	0.020	0.008
	III	**0.211**	**0.192**	0.029	0.032	0.009	0.012	0.024	0
Desert area	I	**0.552**	**0.352**	0.070	0.038	0.047	0.003	0.005	0.007
	II	**0.463**	**0.370**	0.084	0.012	0.020	0	0.001	0
	III	**0.534**	**0.535**	0.060	0.070	0.064	0.001	0.041	0.005
High mountains	I	**0.091**	**0.061**	0.054	0.085	0.035	0.033	0.057	0.028
	II	**0.105**	**0.072**	0.062	0.08	0.062	0.042	0.036	0.101
	III	**0.025**	**0.017**	0.057	0.079	0.017	0.021	0.063	0
Plateau	I	**1.415**	**0.850**	0.183	0.156	0.011	0.009	0.003	0.002
	II	**1.075**	**0.672**	0.205	0.230	0.022	0.008	0	0.003
	III	**1.085**	**0.732**	0.201	0.187	0.036	0.007	0.002	0.001

5.5 Results of Biorthogonal Wavelet Design

In case of texture discrimination, features are calculated at different resolution levels therefore, reconstruction of signal may not be necessary. Hence, condition for perfect reconstruction imposed on scaling coefficients can be relaxed and extra degree of freedom can be used in locating the maxima of distinguishability function. Following are the additional conditions for the design of biorthogonal wavelet system [37].

- Total length of analysis filters (H_o,H_1) should be multiple of four.
- The analysis filters (H_o,H_1) should be FIR filters and must be of even or odd length at the same time. When they are of even length, H_o should be symmetric and H_1 anti-symmetric. When they are of odd length, both of them should be symmetric.
- Condition of Perfect Reconstruction: Product filter $P_o(z)$ can be defined as $H_o(z)G_o(z)$. Similarly, $H_1(z)G_1(z)$ for $P_1(z)$. (4.12) implies that for perfect reconstruction:

$$P_o(z) - P_o(-z) = 2z^{-l} \tag{5.1}$$

In this design example, we have kept the total length $N_o+N_1=8$. Hence, possible lengths of analysis filters can be $(N_o,N_1) =\{(2,6)\ (3,5)\ (5,3)\ (6,2)\ \}$. In case of symmetric filters, zeros can appear either in pairs for complex conjugate or in quadruples for complex conjugate and its reciprocals. Therefore, at least one zero is placed essentially at z= -1 for the existence and convergence of wavelet function, along with other necessary constraints for the construction of biorthogonal wavelet.

Optimization process for different combinations of (N_o,N_1) listed above was executed for three decomposition levels. Detailed analysis of results is listed in Table 5.4 in comparison with corresponding biorthogonal families. It is evident from the values of $J(h)$ that by relaxing the condition for perfect reconstruction, we have achieved more

distinguishability between the texture images. Best results have been obtained by using App._rbior2.2 *(J(h)=5.2639)* in comparison with other biorthogonal wavelet families.

Table 5.4 Results of Optimization Process

S/No	Family	Length of filter (N_{LP},N_{HP})	Regularity (L_{LP},L_{HP})	Obj. function J(h)
Optimized biorthogonal wavelet				
1	App._bior1.3	2,6	1,3	0.0841
2	App._bior2.2	3,5	2,2	4.3257
3	App._rbior3.1	6,2	3,1	0.1914
4	**App._rbior2.2**	**5,3**	**2,2**	**5.2639**
Cohen-Daubechies-Feauveau Family CDF				
5	bior1.3	2,6	1,3	0.1515
6	bior2.2	3,5	2,2	0.1204
7	rbior3.1	6,2	3,1	0.1404
8	rbior2.2	5,3	2,2	0.0896
9	bior2.4	9,3	4,2	0.0924
10	bior2.6	13,3	6,2	0.1457
11	bior2.8	17,3	8,2	0.1835
12	rbior2.4	3,9	2,4	0.0532
13	rbior2.6	3,13	2,6	0.0870
14	rbior2.8	3,17	2,8	0.1527

Increasing the length of the wavelet or regularity does not help in improving the distinguishability. Therefore, we have restricted the design process to shorter lengths to avoid un-necessary computations. Response of analysis and synthesis scaling function are shown in Figure 5.5. We have used the cascade algorithm up to eight iterations for the generation of analysis/synthesis scaling function [37]. Results listed in Table 5.4 show that odd length filters with equal number of zeros at ?=p perform better than even length filters. Analysis and wavelet filter coefficients are given in Table 5.5 along with their frequency responses shown in Figure 5.6.

Table 5.5 Filter Coefficients of Optimized Scaling and Wavelet Filter.

n	1	2	3	4	5
$h_o(n)$	-0.1313	0.2570	0.7480	0.2570	-0.1313
$h_1(n)$	0.2527	-0.4946	0.2527	-	-

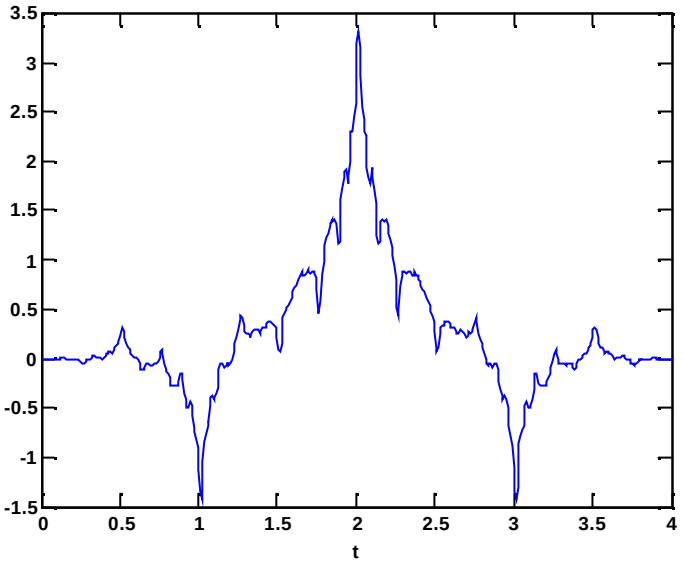

(a) Analysis Scaling Function by Successive Approximation

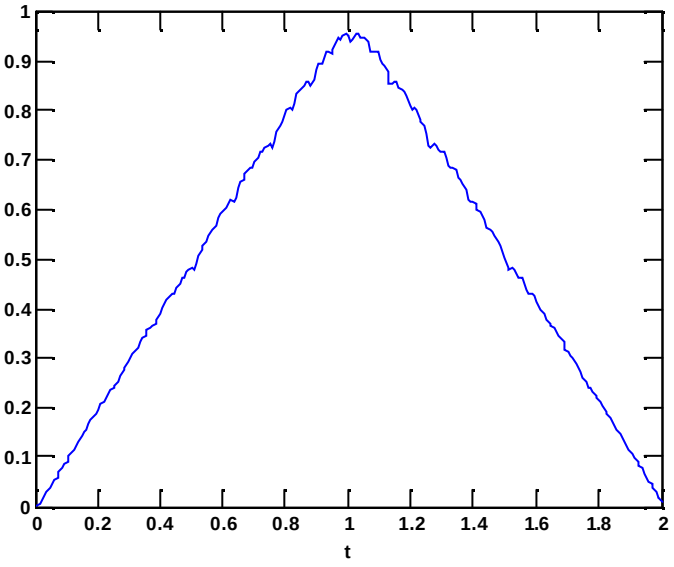

(b) Synthesis Scaling Function by Successive Approximation

Figure 5.5 Responses of Designed Biorthogonal (rbior2.2) Scaling Function $f_o(t)$

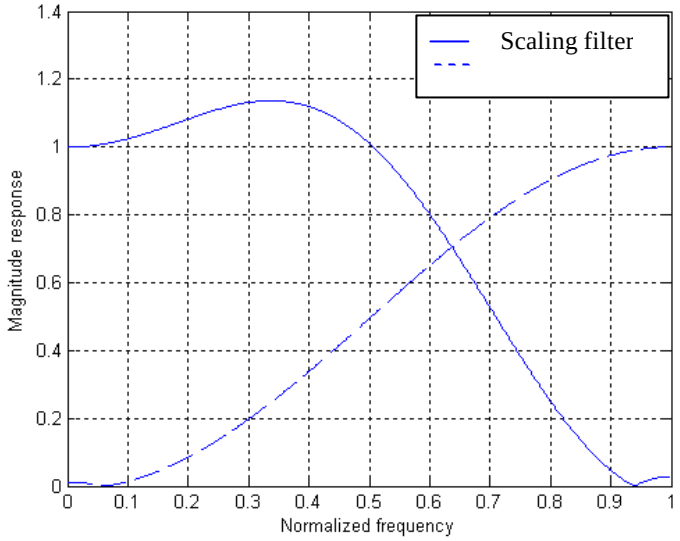

Figure 5.6 Magnitude Responses of Appropriate Biorthogonal Scaling and Wavelet Filters

In case of maximally flat linear phase FIR wavelets [36], $H_o(z)$ is taken to be a factor of maximally flat half-band filter in which all the degrees of freedom have been used to impose maximum number of zeros at *?* = *p*. In our design we used these extra degrees of freedom for best possible texture discrimination. The distinguishability function expressed by (4.8) maximizes the difference between two texture images. Therefore, we kept the texture image of cultivated region Figure 5.1(a) as reference and used rest of the images shown in Figure 5.1 to compute the values of distinguishability function. Results of up to three decomposition levels are listed in ascending order with reference to image of grass are given in Table 5.6. Comparison of distinguishability function $d(I_g , I_n)$ using proposed appropriate biorthogonal wavelet with other well known biorthogonal wavelets shows that the results obtained are superior in terms of achieving distinguishability

between the texture images. The proposed design problem can be extended to higher lengths of wavelets in a similar way and for different set of texture images.

5.6 Texture Discrimination Using Minimum Distance Classifier

Numerous clustering and classification approaches are available, but we have used the minimum distance classifier will be used to illustrate the effectiveness of the proposed biorthogonal wavelet optimization methodology for robust feature extraction [33]. Output detailing coefficients at different resolution levels were used to form a feature vector. In order to decide the efficiency of optimized wavelet for texture discrimination, the performance of a simple minimum distance classifier was evaluated. It is based upon the assumption that each pattern class $\mathbf{W_k}$ is represented by a prototype pattern $\mathbf{Z_k}$ (class center).

Table 5.6 Performance Comparison of Distinguishability Function $d(T_g, T_i)$ for Different Texture Images in Comparison with Texture Image of Cultivated Region

Class type	Samples	**App rbio2.2**	Bior1.3	Bior2.2	Bior2.4	Bior2.8	Rbio1.3	Rbio2.2
Cultivated region	I	0	0	0	0	0	0	0
	II	0	0.041	0.018	0	0.008	0	0
	III	0.002	0.004	0.002	0.003	0	0.001	0.002
Low mountain	I	0.9249	0.009	0.006	0.006	0.006	0.003	0.005
	II	0.5166	0.001	0.007	0.005	0.005	0.002	0.004
	III	0.7147	0.001	0	0.004	0.007	0.003	0.004
Desert area	I	1.7597	0	0.032	0.038	0.006	0.002	0
	II	1.1289	0.001	0.025	0.045	0.005	0.003	0
	III	1.7941	0.02	0.024	0.044	0.07	0.002	0
High mountains	I	0.2727	0.003	0.003	0.007	0.004	0.004	0.002
	II	0.2194	0.03	0.002	0.008	0.005	0.003	0.003
	III	0.2789	0.02	0.003	0.006	0.004	0.005	0.001
Plateau	I	4.084	0.02	0.035	0.045	0.021	0.01	0.02
	II	3.0823	0.06	0.045	0.054	0.028	0.02	0.02
	III	2.367	0.02	0.039	0.036	0.019	0.01	0.01

The minimum distance classifier assigns the pattern **X** of unknown classification to the class $\mathbf{W_k}$, if the distance $\mathbf{D_k}$ between **X** and $\mathbf{Z_k}$ was minimum among all possible class prototypes, where the Euclidean distance $\mathbf{D_k}$ is defined by (5.2).

$$D_k = \|X - Z_k\| = \sqrt{\sum_{j=0}^{N-1} (x_j - z_{j,k})^2} \tag{5.2}$$

In practice, the true class centers $\mathbf{Z_k}$ are unknown. In our case (supervised classification) each class center was estimated by using the mean of the training samples for each class by using:

$$Z_k = \frac{1}{N} \sum_j X_j \tag{5.3}$$

We have obtained an appropriate wavelet basis which provides the best possible discrimination between different textural regions shown in Figure 5.1 in comparison with cultivated region Figure 5.1 (a). The results of designed wavelet in comparison with different orthogonal and biorthogonal families are given in Table 5.1 and 5.4, which shows distinct class separation. Designed orthogonal wavelet with length four performs best amongst the designed wavelets. Figure 5.7 shows the plot of mean values of distinguishability function of the designed orthogonal wavelet in comparison with Daubechies wavelet (length four and eight).

Horizontal axis corresponds to different classes and the vertical axis shows the magnitude of Distinguishability function. Sharp change in the curve of designed wavelet corresponds to higher class separation and flatter curve shows little change in the magnitude of Distinguishability function. Each texture image of all the classes were broken down into 100 overlapping sub-images of dimension 128x128 for classification purpose.

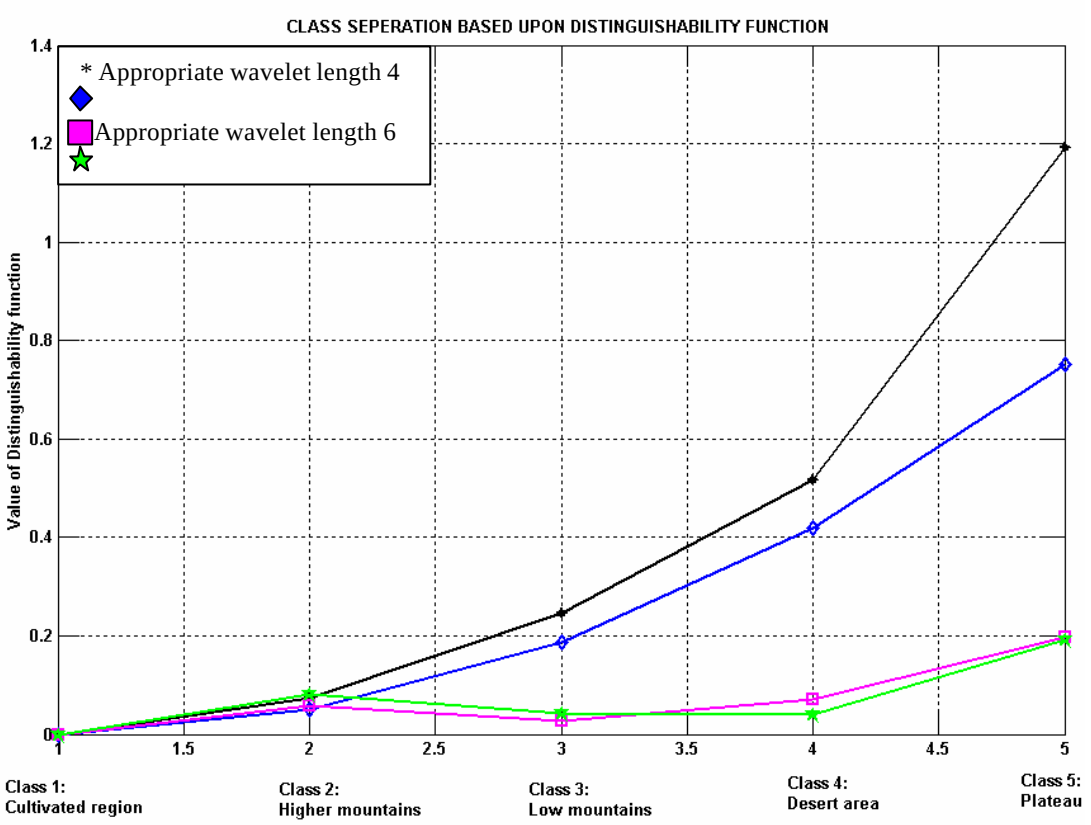

Figure 5.7 Performance Comparison of Designed and Daubechies Wavelet for the Mean Values of Distinguishability Function for Different Classes.

Each image was decomposed to three decomposition levels using designed wavelet and other wavelets in order to form a 9 dimensional feature vector. Classification was performed using minimum distance classifier, which assigns the pattern of unknown classification to the class having minimum distance among all possible class prototypes.

Classification results using minimum distance classifier are given in Table 5.7, which show that the appropriate orthogonal wavelet with length four performs best amongst others in terms of texture discrimination.

Table 5.7 Classification Results

Wavelet	% Correct classification
Appropriate wavelet (N=4)	85
Appropriate wavelet (N=6)	81
Daubechies wavelet (N=4)	72
Daubechies wavelet (N=20)	69
Symlet wavelet	72

5.7 Application in Medical Imaging

The Computer aided diagnostics CAD has become one of the major research subject in medical imaging and diagnostics radiology. The basic concept of CAD is to provide the computer aided output as a second opinion to assist the radiologists. It can improve the diagnostic accuracy and reduces image reading and interpretation time. CAD tools can be designed with known clinical need such as analysis of difficult to interpret images, shortage of expertise, cost effective utilization of available resources [67].

In CAD and imaging modalities, the application of texture analysis in diagnostic interpretation of radiological images has become rapidly expanding field of research. Texture analysis is a popular and important area of image processing and it has wide applications in medical imaging. Various texture analysis methods have been developed to analyze and classify various tissue patterns including prostrate cancerous lesions [69], liver lesions [70], brain tumors [71] skin carcinomas [72] etc.

Skin cancers are the most common form of cancers in humans. The American Cancer Society estimates that more than 700,000 new skin cancers are diagnosed annually in the alone. Skin cancers can be classified into melanoma and non-melanoma. Although melanomas are much less common than non-melanomas, they account for most of the mortality from skin cancers. Detection of malignant melanoma in its early stages considerably reduces morbidity and mortality. Early detection also saves hundreds of

millions of dollars that otherwise would be spent on the treatment of advanced diseases [68].

5.7.1 Design of a Wavelet for the Analysis of Skin Carcinomas

In order to search for small, subtle, masked and infrequent abnormalities, automated method of diagnosis is required with the aim of improving diagnostic capabilities. Therefore, we propose a scheme for the design of a wavelet bases for discrimination of infected skin tissues from the healthy ones using genetic algorithm. In the genetic optimization process, design parameters of wavelet are optimized according to the characteristics of the texture images under defined set of constraints. In this technique, single mother wavelet function was designed using the technique developed in Section 4.3 and 4.4 for the analysis of skin cancer and pigmented lesions in dermoscopical texture images. Experimental analysis has been carried out using set of infected tissue sample images and wavelet function was optimized to illustrate the discrimination ability of the proposed technique.

There are three major types of skin cancers, which comprises more than 99 percent of all skin cancers and are named based on the type of skin cell. Basal Cellcarcinoma (BCC) from the basal cell, Squamous Cell-Ccarcinoma (SCC) from the squamous cell, and Melanoma from the melanocytes. BCC and SCC are also called nonmelanoma skin cancers. For all of these skin cancers, the cure rate is always higher if detected and treated early. Also, early treatment is much simpler, less invasive and less expensive. Figure 5.8 shows the data set of twenty infected skin lesions comprising on

BCC, SCC and Melanoma lesions. Images 1- 6, 7-13 and 14-20 form left to right shows BCC, SCC and Melanoma lesions respectively.

Figure 5.8 Twenty Images of Skin Lesions

5.7.2 Results of Designed Wavelet for Skin Carcinomas

Suitable wavelet was designed by selecting randomly two samples from each category shown in Figure 5.9 by maximizing the constrained objective function given in (4.19).

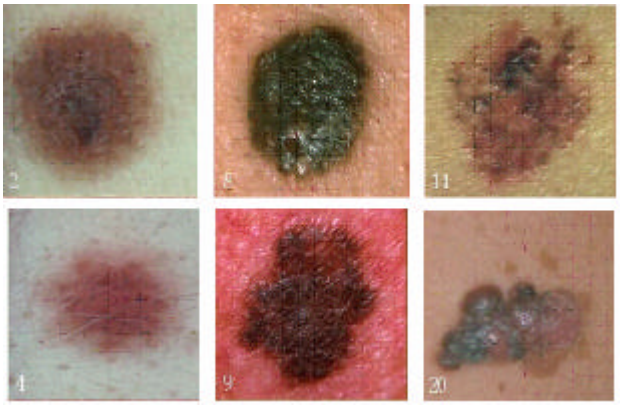

Figure 5.9 Samples of Infected Skin Lesions Used for the Design of Wavelet

The results of objective function *J(h)* of designed wavelet are given in Table 5.8 in comparison with different orthogonal and biorthogonal wavelet families.

Table 5.8 Results of *J(h)* for Designed and Different Wavelet Families

Wavelet family	Objective function *J(h)*	Wavelet family	Objective function *J(h)*
Designed wavelet (N=4)	**0.9866**	Symlet N=4	0.6892
Daubechies (N=4)	0.7519	Bior2.2	0.7123
Daubechies (N=6)	0.7921	Bior4.4	0.7388
Daubechies (N=8)	0.7758	Bior6.8	0.7265
Daubechies (N=10)	0.7819		

Therefore, it can be concluded from the results that orthogonal Appropriate wavelet of length (N=4) is best suited amongst other wavelets for given set of texture images. Proposed filter coefficients are given in Table 5.9.

Table 5.9 Scaling Filter Coefficients of Designed Wavelets for the Analysis of Skin Carcinomas

N	0	1	2	3
Designed wavelet N=4	0.0954	0.3253	0.5955	0.1746

5.8 Summary

In this chapter, we have simulated and designed the suitable wavelet based upon the performance metric given (4.20) using necessary and sufficient constraints by using remotely sensed texture images of Pakistan. The designed appropriate wavelet is highly dependant upon the texture images used in the offline design process. It is evident from the results of distinguishability function and classification that orthogonal wavelet of length four performs better amongst the designed orthogonal and biorthogonal wavelets in terms of discrimination between different texture images and computation complexity.

CHAPTER 6

CONCLUSION AND FUTURE WORK

6.1 Conclusion

Texture analysis and discrimination is one the most challenging parts of a comprehensive vision system. Accurate segmentation and classification of a given scene is highly dependant on robust discrimination technique without which any further processing and extraction of precise information in a real world scene is not possible. Therefore, it is not surprising to see the attention of researchers on this topic for the last thirty years and one can find a whole surfeit of methods for segmentation of textured regions in the literature. However, the more challenging problem is to find the best method which can provide better discrimination and low computational complexity.

In this research work, we have proposed a scheme for the design of appropriate wavelet bases for best possible texture discrimination under defined set of constraints. We have used set of remotely sensed texture images of Pakistan for the design of appropriate wavelet. The design objective was to search for unknown wavelet coefficients that will maximize the value of distinguishability function by moving the feature vectors apart. Results of texture discrimination of the designed wavelet are given in the previous chapter in comparison to other wavelet families. The results show that the designed wavelet of length four performs best amongst all other wavelets.

We have restricted the wavelet scaling function length equal to four and six based upon the texture discrimination results. Increase in length of wavelet does not help in

achieving better discrimination, but it would increase undue computation load. Based upon overall results we have come to following conclusion:

- Higher number of vanishing moments would not necessarily yield optimum texture discrimination. In stead extra degree of freedom should be used in locating the maxima of objective function.
- Shorter length filters with reasonable frequency response generally yield better results in terms of texture discrimination.

Appropriate wavelet design method is dependant upon the set of texture images used for design purpose. Therefore, this algorithm can easily be modified for other type of texture images as well.

6.2 Future Work

From the texture point of view, a comprehensive mathematical model for textures is highly desirable. The main issue is whether we can find a general mathematical model for all sorts of textures; or else we will have to partition the space of all textures into some application domains. Then for each one of these applications find the right model. Having pursued such model(s) we will be able to find the optimal solutions for each application area. We have proposed the technique for the design of wavelet function using genetic optimization. The proposed technique gives improved results in comparison to other wavelet families. Further work may be carried out by using different dissimilarity measures and wavelet packets, which gives greater control over the partitioning of time frequency plane.

REFERENCES

[1] M. Tuceyran and A.K. Jain, "Texture Analysis," *Handbook of Pattern Recognition and Computer Vision*, C.H. Chen, L.F. Pau and P.S.P. Wang (Eds.), chapter 2, pp. 235-276, World Scientific, Singapore, 1993.

[2] R. M. Haralick. "Statistical and Structural Approaches to Texture," *Proceedings of the IEEE*, vol. 67(5), pp. 786-804, May 1979.

[3] S Theodoridis and K Koutroumbas, *Pattern Recognition*, Academic press 1998.

[4] W. Pratt, *Digital Image Processing*. John Wiley and Sons, 1991.

[5] K. I. Laws, "Texture Image Segmentation," Ph.D. Thesis, Univ. of Southern California, USA 1980.

[6] M Sharma, Markou and S Singh, "Evaluation of Texture Methods for Image Analysis," *Intelligent Information Systems Conference, Seventh Australian and* New Zealand, 2001.

[7] J.Y.Hsiao and Alexander A. Sawchuk. "Supervised Textured Image Segmentatio n Using Feature Smoothing and Probabilistic Relaxation Techniques," *IEEE Transactions on Pattern Analysis and Machine Intelligence*, vol. 11(12) pp. 1279-1292, Dec 1989.

[8] J.M. Coggins and A.K. Jain, "A Spatial Filtering Approach to Texture Analysis," *Pattern Recognition Letters*, vol. 3, no. 3, pp. 195–203, 1985.

[9] R. Azencott, Jia-Ping Wang, and Laurent Younes, "Texture Classification Using Windowed Fourier Filters," *IEEE Transactions on Pattern Analysis and Machine Intelligence*, vol. 19, no. 2, pp. 148-153 February 1997.

[10] T. Hsu, A.D. Calway and R. Wilson, "Texture Analysis Using Multiresolution Fourier Transform," *Proc. 8th Scandinavian Conference on Image Analysis* May 1993.

[11] A.K Jain and F.Farrokhnia, "Unsupervised Texture Segmentation using Gabor Filters," *Pattern Recognition*, vol. 24 pp. 1167-1186,1991.

[12] A.C Bovik., M. Clark & W.S. Geisler "Multi-channel Texture Analysis Using Localized Spatial Filters," *IEEE Trans. Pattern Analysis and Machine Intelligence.* vol. 1, pp. 55–73. 1990.

[13] T. P. Weldon, Williams E. Higgins and Dennis F. Dunn, "Gabor Filter Design for Multiple Texture Segmentation," *Opt.Eng SPIE* October 1996.

[14] N.N Kachouie. & Javad Alirezaie. "Optimized Multi-Channel Filter Bank with Flat Frequency Response for Texture Segmentation," *EURASIP Journal on Applied Signal Processing*, vol. 12, pp. 1834-1844. 2005.

[15] S. E. Grigorescu, N. Petkov, and Peter Kruizinga, "Comparison of Texture Features Based on Gabor Filters," *IEEE Trans. on Image Processing*, vol. 11, no. 10, pp. 1160-1167, October 2002

[16] P.P. Vaidyanathan, "Multirate Digital Filters, Filter banks, Polyphase Networks and Applications," *Proc. of IEEE*, vol. 78, January 1990.

[17] P.P. Vaidyanathan, *Multirate Systems and Filter banks*. Prentice Hall, New Jersey 1993.

[18] M. Vetterli, "Filter Banks Allowing Perfect reconstruction" *Signal Processing*, Vol. 10 pp. 219-244 Apr 1986.

[19] M. Vetterli, "A Theory of Mult-irate Filter Banks," *IEEE Trans. Acoust. Speech Signal Processing*, vol. 35, pp. 356-372, March 1987.

[20] T. Q. Nguyen and P.P. Vaidyanathan, "Two Channel Perfect Reconstruction FIR QMF Structures which Yield Linear Phase Analysis and Synthesis Filters," *IEEE Trans. Acoust. Speech Signal Processing*, vol. 37, pp. 676-690, May 1989.

[21] B. R. Horng and A. N. Willson, "Lagrange Multiplier Approach to the Design of Two Channel Perfect Reconstruction Linear Phase FIR Filter Banks," *IEEE Trans. Signal Processing*, vol. 40, no 2, pp 364-374, February 1992.

[22] J. Shyu and Yuan-Chih Lin, "A New Approach to the Design of Discrete Coefficient FIR Digital Filters," *IEEE Trans. Signal Processing*, vol. 43, no 1, pp 310-314, January 1995.

[23] T. Wang and Benjamin W. Wah, ``Performance Measures and Lagrange Multiplier Methods to Two-Band PR-LP Filter Bank Design," *Proc. IEEE Int'l Conf. on Acoustics, Speech and Signal Processing*, vol. 3, pp. 1461-1464, May 1998.

[24] J. D. Johnston, "A Filter Family Designed for QMF Filter Banks," *Proc. IEEE Int Conf Acoust Speech and Signal Proc*. pp 291-294, April 1980.

[25] C. D Creusere and Sanjit K Mitra, "A Simple Method for Designing High Quality Prototype Filters for M Band Pseudo QMF Banks," *IEEE Trans. Signal Processing*, vol. 43, no 4, pp 1005-1007, April 1995.

[26] Oppenheim A.V, R.W.Schaffer and J.R.Buck, *Discrete Time Signal Processing*, Prentice Hall, New Jersey, 2001.

[27] S. Jayasimha and C.G. Hiremath, "Pseudo QMF Banks with Near Equiripple Performance," *IEEE Trans. Signal Processing*, vol. 46, no 1, pp 209-214, January 1998.

[28] M.A.Chaudhry and M.N.Jafri, "Optimal Design of QMF Filter Banks Based on Max-flat Polynomial for Texture Analysis," *8th IEEE International Multi-topic Conference INMIC* Dec 2004, Lahore, Pakistan.

[29] M.A.Chaudhry, M.N.Jafri and Muid Mufti, "Optimal Design of Filter Banks for Texture Discrimination," *WSCG International Conference on Computer Graphics* 4th Feb 2005, Plzen Czech Republic.

[30] A. Mahalanobis and H.Singh, "Application of Correlation Filters for Texture Recognition," *Appl. Opt.* vol. 33 pp. 2176-2179, 1994.

[31] M. Unser, "Local Linear Transforms for Texture Measurement," *Signal Processing* vol. 11, pp. 61-79, 1986.

[32] T. Randen and J.H. Husoy, "Texture Segmentation Using Filters with Optimized Energy Seperation," *IEEE Trans. Image Processing*, vol. 8, no 4, pp 571-582, April 1999.

[33] K. Fukunaga, *Statistical pattern recognition*, 2nd Edition New york Academic 1990.

[34] T. Randen and J.H. Husoy, "Filtering for Texture Classification: A Comparative Study," IEEE *Trans. Pattern Analysis and Machine Intelligence*, vol. 21, no 4, pp 291-310, April 1999.

[35] S.Mallat, "A Theory of Multiresolution Signal Decomposition: The Wavelet Representation," *IEEE Trans. Pattern Analysis and Machine Intelligence*, vol. 11, no 21, pp. 674-693, Mar. 1989.

[36] I. Daubechies, "Orthonormal Bases of Compactly Supported Wavelets," *Communication on Pure and Applied Mathematics*. 41:909-996, Nov 1988.

[37] R. A. Gopinath and C. S. Burrus, *Wavelet transform and Filter banks*. In C. K Chui, Editor, Wavelets: A Tutorial in Theory and Applications, pp 603-655, Academic press, San Diego, CA 1992.

[38] A. Cohen, I. Daubechies and J.C. Feauveau, "Biorthogonal Bases of Compactly Supported Wavelets," *Communication on Pure and Applied Mathematics*, vol. 45, pp. 485-560, 1992.

[39] T. Chang and C.C.J. Kuo, "Texture Analysis and Classification with Tree Structured Wavelet Transform," *IEEE Trans. Image Processing*, vol. 2 no 4, pp 429-441, October 1993.

[40] M. Unser and M. Eden, "Multiresolution Feature Extraction and Selection for Texture Segmentation," *IEEE Trans. Pattern Analysis and Machine Intelligence*, vol. 11, no 7, pp 717-728, July 1989.

[41] M. Unser, "Texture classification and Segmentation Using Wavelet Frames," *IEEE Tran. Image Processing*, vol.11 No 4, pp 1549-1560, Nov 1995.

[42] A. Laine and J.Fan, "Texture Classification by Wavelet Packet Signatures," *IEEE Trans. Pattern Analysis and Machine Intelligence*, vol. 15, no 11, pp 1189-1190, Nov 1993.

[43] G. Van de Wouwer, P. Scheunders and D. Van Dyck, "Statistical Texture Characterization from Discrete Wavelet Representation," *IEEE Tran. on Image Processing*. vol. 8 no 4, pp 592-598, April 1999.

[44] C. Pun, M, Lee, "Log-Polar Wavelet Energy Signatures for Rotation and Scale Invariant Texture Classification," *IEEE Trans. Pattern Analysis and Machine Intelligence*, vol. 25, no 5, pp 590-603, May. 2003.

[45] K. J. Khouzani and H. Soltanian-Zadeh, "Rotation Invariant Multiresolution Texture Analysis Using Randon and Wavelet Transform," *IEEE Trans. Image Processing*, vol. 14 no 6, June 2005.

[46] G. Fan and Xiang-Gen Xia, "Wavelet Based Texture Analysis and Synthesis Using Hidden Markov Models," *IEEE Trans. Circuit and Systems*, vol 50 no 1, pp 106-120, January 2003.

[47] N. Sebe and Michael Lew, "Wavelet Based Texture Classification," *IEEE Proc. of International Conference on Pattern Recognition*, pp. 1051-4651 ICPR 2000.

[48] A. Mojsilovic, S. Markovic and Popovic, "Texture Analysis and Classification with the Non-separable Wavelet Transform," *IEEE Proc. of International Conference on Image Processing*, pp. 8186-8183 ICIP 1997.

[49] G. Lambert and F. Bock, "Wavelet Methods for Texture Defect Detection," *IEEE Proc. of International Conference on Image Processing*, pp. 8186-8183 ICIP 1997.

[50] A. Mojsilovic, V. Popovic and D. M. Rackov, "On the Selection of an Optimal Wavelet Basis for Texture Characterization," *IEEE Trans. on Image Processing.* vol 9 no 12, pp 2043-2050, Dec 2000.

[51] S. Livens, Image Analysis for Material Characterization. PhD thesis, University of Antwerpens, 1998.

[52] M. Mufti and G. Vachtsevanos, "Fuzzy Wavelet for Feature Extraction and Intelligent Control," *International Journal of Fuzzy Systems*, vol. 5 no. 2, June 2003.

[53] A. Mojsilovic, V. Popovic and S. Markovic, "Characterization of Visually Similar Diffuse Diseases from B-Scan Liver Images using Non-Separable Wavelet Transform," *IEEE Trans. on Medical Imaging*. vol 17, no 4, pp. 1005-1009, August 1998.

[54] A. Mojsilovic, V. Popovic, A. N. Neskovic and A. D. Popovic, "Wavelet Image Extension for Analysis and Classification of Infarcted Myocardial Tissue," *IEEE Trans. on Bio-Medical Imaging*. vol 44, no 9, Sept 1997.

[55] K.K.Simhadari, S.S.Iyengar, R.J.Holyer, M.Lybanon and J.M.Zachary, "Wavelet Based Feature Extraction from Oceanographic Images," *IEEE Trans. on Geosciences and Remote Sensing*. vol 36, no 3, pp 767-778, May1998.

[56] A.Sofou, G.Evangelopoulos and P.Maragos, "Soil Image Segmentation and Texture Analysis: A Computer Vision Approach," *IEEE Trans. on Geosciences and Remote Sensing*. vol 2, no 4, pp. 394-398 Oct. 2005.

[57] W.Taixia and Z.Yunsheng, "The Bidirectional Polarized Reflectance Model of Soil," *IEEE Trans. on Geosciences and Remote Sensing*. vol. 43, no 12, pp 2854-2859, December 2005.

[58] P.Maillard, D.A.Clausi and H.Deng, "Operational Map Guided Classification of SAR Sea Ice Imagery," *IEEE Trans. on Geosciences and Remote Sensing*. vol. 43, no 12, pp 2940-2951, December 2005.

[59] L.Soh and C.Tsatsoulis, "Texture Analysis of SAR Sea Ice Imagery Using Gray Level Co-occurrence Matrices," *IEEE Trans. on Geosciences and Remote Sensing*. vol. 37, no 2, March 1995.

[60] P.Saich and M.Borgeaud, "Interpreting ERS SAR Signatures of Agricultural Crops in Flevoland, 1993-1996," *IEEE Trans. on Geosciences and Remote Sensing*. vol. 38, no 2, March 2000.

[61] K.A.Stankeiwicz, "The Efficiency of Crop Recognition on ENVISAT ASAR Images in Two Growing Seasons," *IEEE Trans. on Geosciences and Remote Sensing*. vol. 44, no 4, April 2006.

[62] D.G.Goodenough, A.Dyk, K.O.Niemann, J.S.Pearlman, H.Chen, M.Murdoch and C.West, "Processing Hyperion and ALI for Forest Classification," *IEEE Trans. on Geosciences and Remote Sensing*. vol. 41, no 6, pp 1321-1331, June 2003.

[63] M.A.Chaudhry, M.N.Jafri, Muid Mufti and M.Akbar, "Optimization of Wavelet Bases for Texture Analysis," *5th IEEE International Symposium on Signal Processing and Information Technology*, December 18-21, 2005, Athens, Greece.

[64] M.A.Chaudhry, M.N.Jafri, Muid Mufti, and M.Akbar "Optimal Design of Biorthogonal Wavelet System for Texture Discrimination Using Genetic Algorithms," *3rd International Conference on Signal Processing, Pattern Recognition and Applications SPPRA*, Feb 2006 Innsbruck Austria.

[65] M.A.Chaudhry, M.N.Jafri, Muid Mufti, and M.Akbar. "Design of Appropriate Wavelet Bases for Texture Discrimination," *Kuwait Journal of Science and Engineering*, vol. 35B, December 2007.

[66] E.D.Goldberg, *Genetic Algorithms in Search, Optimization and Machine Learning.* Addison Wesley Publishing Company Inc 1989.

[67] K. Doi, "Current Status and Future Potential of Computer Aided Diagnosis in Medical Imaging" *British Journal of Radiology*, Vol 78, 2005.

[68] American cancer society,"Cancer Facts and Figures 2002".http://www.cancer.org.

[69] M. A. Tahir, A. Bouridane, F. Kurugollu, and Abbes Amira, "A Novel Prostate Cancer Classification Technique Using Intermediate Memory Tabu Search," *EURASIP Journal on Applied Signal Processing* , vol. 14, no. 7, pp. 2241-2249, 2000.

[70] D.Smutek et at, "Texture Analysis of Hepatocellular Carcinoma and Liver Cysts in Ct Images." *Proceeding of International Multi-conference Signal rocessing, pattern recogntion and applications,* Innsbruck, Austria 2006.

[71] R.A. Brown, M.C. Zlatescu, J.G. Cairncross, and J.R. Mitchell ., "Texture Analysis for Non-invasive Identification of Brain Tumor Genotype from MRI," *International Conference on Visualization, Imaging, and Image Processing VIIP* , September 2005.

[72] L. Xu et al., "Segmentation of Skin Cancer Images," *Journal of Image and Vision Computing ELSEVIER*, vol. 17, no. 2, pp. 65-74, 1999.